

25 **ABSTRACT**

26 The coupling of lake dynamics with the catchment biogeochemistry has been considered the key
27 element controlling primary production in mountain lakes at time scales of a few decades to millennia.
28 Yet, little is known on the effects produced by changes in the morphometry of lakes throughout their
29 ontogeny. Lake Chungará (Central Andean Altiplano, northern Chile) experienced long-term lake-level
30 fluctuations that strongly modified its area:volume ratios, making it an ideal system to explore the
31 relative role that long-term climatic shifts and changes in morphometry play on biosiliceous lacustrine
32 productivity. In this paper we review previous data on percent content of total organic carbon, total
33 inorganic carbon, total nitrogen, total biogenic silica, isotopic composition of organic matter,
34 carbonates, and diatom frustules, as well as on the abundances of the chlorophycean *Botryococcus*
35 *braunii* in this lake for the period 12,400-1,300 cal yr BP. We also include new data on organic carbon
36 and biogenic silica mass accumulation rates and diatom assemblages composition of an offshore core
37 dated with ^{14}C and U/Th.

38 Biosiliceous productivity was primarily influenced by shifts in allochthonous nutrient inputs related
39 to precipitation variability. Humid phases dated at c. 12,400 to 10,000, 9,600 to 7,400 and 3,550 to
40 1,300 cal yr BP, coincide with periods of elevated productivity. Conversely, falls in productivity were
41 recorded during arid phases dated at c. 10,000 to 9,600 and 7,400 to 3,550 cal yr BP (Andean mid-
42 Holocene Aridity Period). Yet, morphometry-related in-lake controls provoked that there was not a
43 linear response of productivity to precipitation variability. During the late Glacial to early Holocene,
44 lowstands facilitated complete water column mixing, prompting the episodic massive blooms of a large
45 centric diatom, *Cyclostephanos* cf. *andinus*. Irrespective of aridity, moderate productivity could
46 therefore be maintained by this phenomenon of morphometric eutrophy during the early history of the
47 lake. The subsequent net increase in lake-level introduced modifications in the area of the epilimnion
48 sediments versus the total volume of the epilimnion that prevented complete overturn. Surpassing a
49 certain depth threshold at c. 8,300 cal yr BP caused the cessation of morphometric eutrophy
50 conditions associated with the *Cyclostephanos* cf. *andinus* superblooms. After 7,300 cal yr BP, the
51 lake experienced a decrease in biosiliceous productivity and a change of state that involved a stronger

52 dependence on precipitation variability, a shift to a bicarbonate-dominated system, and a lesser
53 contribution of diatoms to total primary productivity. Our results show that interpretation of lacustrine
54 paleoproductivity records as paleoclimatic archives need to take into account the effects of changes in
55 morphometry associated with the ontogeny of lakes.

56

57

58

59

60

61 **Keywords:** lake paleoproductivity, lake ontogeny, laminated sediments, diatoms, Andean Altiplano,
62 Holocene

63

64 1. INTRODUCTION

65 Photosynthetic activity in periodically stratified lakes is generally restricted by phosphorous and
66 nitrogen concentrations in the epilimnion, because the waters underneath, although richer in these
67 limiting nutrients, do not receive sufficient light to sustain significant primary productivity (Sterner,
68 2008). This vertical segregation is usually eliminated when deep mixing of the water column brings the
69 bottom nutrient-rich waters to the euphotic zone. Nutrient and mixing gradients are therefore primary
70 drivers of phytoplankton dynamics and productivity in aquatic ecosystems (Winder & Hunter, 2008).
71 Morphometric characteristics of the lake basin influence the total epilimnion volume and the degree of
72 water column mixing and, therefore, can be an important influence on lake productivity (Imboden &
73 Wüest, 1995; Wetzel, 2001).

74 The relative role that lake morphology plays in affecting productivity likely varies geographically and
75 through time. In a classical paper, Rawson (1955) reviewed data from a series of large lakes and
76 concluded that lake morphometry was a determinant factor in lacustrine productivity, a result that
77 could not be reproduced by Brylinsky & Mann (1973), who considered morphometry as relatively
78 unimportant in affecting phytoplankton production. These ecological studies relied on space-for-time
79 substitution approaches (Smol, 2008) and did not take into account changes in productivity that could
80 be associated with modifications in the morphology of an individual lake over long periods of time.
81 Moreover, in spite of evidence generated by Quaternary paleoecologists (Engstrom et al., 2000),
82 many limnologists still assume a traditional model of progressive eutrophication of lakes over time
83 (Deevey, 1955). Temporal change in phytoplankton communities and their function is a time-scale
84 dependent process whose study has largely ignored the long-term variability resulting from lake
85 ontogeny (Anderson, 1995). Data analyses on broad time scales provide new insights on the role that
86 both climate and local physiographic factors can have in affecting the productivity of lake systems.
87 Disentangling the relative importance of these two factors is required in Quaternary paleoclimatic
88 reconstructions that rely in part on the study on changes in paleoproductivity inferred from biosiliceous
89 proxy data (e. g., Johnson et al., 2004; Mackay, 2007; Castañeda et al., 2009).

90 Lakes in the Central Andean Altiplano experienced strong lake-level fluctuations during the Late
91 Quaternary that altered their surface area:volume ratios (Placzek et al., 2009). This variation makes
92 them ideal systems to explore the relative role that long-term climatic shifts and changes in
93 morphometry play in affecting lacustrine productivity. The millennial scale moisture balance of the
94 Atlantic-Amazon-hydrologic system is strongly influenced by precessional changes in solar insolation
95 (e. g. Rowe et al., 2002), although changes in Equatorial Pacific sea-surface temperature (SST) and
96 El Niño-Southern oscillation (ENSO) variability also may have played a role (Polissar et al., 2013). All
97 of these factors contributed to changes in lake-levels that, in turn, affected the composition of
98 planktonic communities (e. g. Tapia et al., 2003). In spite of this, very little is known regarding the
99 effects of long-term lake-level variability on functional properties, such as lacustrine productivity, of
100 regional limnological systems.

101 Lake Chungará (Central Andean Altiplano, northern Chile) is a surficially closed lake that has
102 undergone significant changes in water level in the last 12,400 years (Sáez et al., 2007). Due to its
103 complex bottom topography, these changes produced important modifications in the surface:volume
104 ratio during its ontogeny, making it a good system to test the relative importance that climate and
105 morphometric characteristics of the lake have on primary productivity variation. There is a former
106 appreciable knowledge of the main changes that occurred in the lake since the Late Glacial based on
107 multiproxy evidence. These included sedimentary facies characterization (Sáez et al., 2007), isotopic
108 composition of bulk organic matter ($\delta^{13}\text{C}_{\text{org}}$, $\delta^{15}\text{N}_{\text{org}}$; Pueyo et al., 2011), carbonates ($\delta^{18}\text{O}_{\text{carbonate}}$,
109 $\delta^{13}\text{C}_{\text{carbonate}}$; Pueyo et al., 2011), and diatom frustules ($\delta^{18}\text{O}_{\text{diat.}}$, $\delta^{13}\text{C}_{\text{diat.}}$; Hernández et al., 2008, 2010,
110 2011, 2013), as well as a moisture balance reconstruction based on magnetic susceptibility, X-ray
111 Fluorescence (XRF), X-ray Diffraction (XRD), Total Carbon and Total Organic Carbon (TC and TOC),
112 Biogenic Silica (BSi) and grey-colour curve of the sediment data (Giralt et al., 2008). But, in spite of
113 the large number of proxies analyzed, an overall picture on the causes behind changes in
114 paleoproductivity in the lake is still lacking.

115 In this paper we integrate these previous and new (diatom assemblages composition, organic
116 carbon and biogenic silica mass accumulation rates) multiproxy data on the paleoenvironmental
117 evolution of Lake Chungará, to develop an evolutionary model of long-term productivity trajectories in

118 a high altitude tropical lake. We also study the relationship between changes in productivity and the
119 main climatic events recorded in the Central Andean Altiplano, as well as the potential role that
120 changes in lake morphometry could have also played. We show how the imprinting of primary climatic
121 forcing signals in the sedimentary record is decisively modulated by the effects of changes in the
122 morphometry of the basin throughout the ontogeny of the lake.

123

124 **2. STUDY SITE**

125 *2.1 Physiographic and limnological features*

126 Lake Chungará (18°15' S, 69°09' W, 4,520 m a.s.l., Fig. 1) was formed between 15,000 and 17,000
127 yr BP after the partial collapse of the Parinacota volcano (Hora et al. 2007; Sáez et al., 2007). The
128 lake has a maximum length of 8.75 km, a maximum water depth of 40 m, a surface area of 21.5 km²,
129 and a volume of 400 x 10⁶ m³ (Mühlhauser et al., 1995; Herrera et al., 2006). The western and
130 northern lake margins are steep, whereas the eastern and southern margins are gentle, forming
131 extensive shallow (less than 7 m deep) platforms (Fig. 1B). The main inlet to the lake is the Chungará
132 small stream (300-460 l s⁻¹), while the main water loss is by evaporation (3.10⁷ m³ yr⁻¹). The
133 groundwater outflow to the near Cotacotani lakes has been estimated as about 6-7 10⁶ m³ yr⁻¹
134 (Risacher et al., 1999; Dorador et al., 2003).

135 Lake Chungará is a cold-polymictic and moderately saline lake, which thermally stratifies from
136 January to April (Mühlhauser et al., 1995). It contains 1.2 g l⁻¹ of Total Dissolved Salts, with a
137 conductivity ranging between 1,500 and 3,000 µS cm⁻¹, and a water chemistry of Na-Mg-HCO₃-SO₄
138 type (Mühlhauser et al., 1995; Dorador et al. 2003). The lake has been classified as oligo-mesotrophic
139 or meso-eutrophic according to chlorophyll-a concentration and photosynthetic activity, respectively
140 (Mühlhauser et al., 1995). Most of the primary productivity is by diatoms, but cyanobacteria and
141 chlorophyceans contribute more during spring and summer (Dorador et al., 2003; Márquez-García et
142 al., 2009). Large concentrations of phosphorous were measured at present (Mühlhauser et al., 1995),
143 but the lake is limited by nitrogen (Dorador et al., 2003; Márquez-García et al., 2009).

144 The lake receives precipitation from the Atlantic Ocean. Annual rainfall in the Chungará region is
145 about 350 mm yr⁻¹, but the range is variable (100-750 mm yr⁻¹). Mean temperature is 4.2°C. Humidity
146 in the region is advected from the Amazon Basin by the South American Summer Monsoon (SASM),
147 which is linked to the Intertropical Convergence Zone (ITCZ) (Zhou & Lau, 1998). The wet season
148 occurs during the austral summer months, when a weak easterly flow prevails over the Altiplano as a
149 consequence of the southward migration of the subtropical jet stream and the establishment of the
150 Bolivian High Pressure system (Baker et al. 2005; Garreaud et al. 2009; Polissar et al., 2013). In
151 addition, a significant fraction of the inter-annual changes in summer precipitation is currently also
152 related to ENSO (Garreaud et al., 2003).

153 2.2 *The lake sedimentary infill*

154 A 3D depositional model based on seismic imagery and sedimentary facies analyses of 15
155 sediment cores identified a total of 6 sedimentary units composed of 7 offshore, 3 littoral-nearshore,
156 and 2 volcanoclastic facies (Sáez et al., 2007) (Fig. 1C). Sediments in the offshore-deepest central
157 plain are made up of laminated (Unit 1) and non-laminated diatomaceous oozes with interbedded
158 tephra layers (Unit 2). The diatomaceous laminated sediments of Unit 1 show rhythmites made up of
159 triplets (4 to 24 yr) of white, light- and dark-green laminae (Hernández et al., 2008, 2011) (Fig. 2).
160 Green laminae are composed of a mixture of the euplanktonic diatom *Cyclostephanos andinus*
161 (always smaller than 50 µm), diatoms of the *Discostella stelligera* complex, and a diverse mixture of
162 tychoplanktonic and benthic diatoms. White laminae show an almost monospecific composition of very
163 large valves of *Cyclostephanos andinus* (>50 µm), which resulted from the deposition of massive
164 short-term blooms of this taxon. These superblooms have been interpreted as triggered by strong
165 influx of nutrient-rich waters from the lake bottom to the photic zone or, less frequently, by nutrient
166 inputs associated with increased runoff (Hernández et al., 2011). The dark laminae are considered to
167 represent the background limnological conditions. The diatomaceous oozes of Unit 2 show no
168 lamination or indication of massive short-term blooms of large *Cyclostephanos andinus*.

169

170 3. MATERIALS AND METHODS

171 In November 2002, 15 sediment cores up to 8 m long were retrieved from the lake with a
172 Kullenberg corer. From the core lithostratigraphic correlation, a composite core spanning the whole
173 sedimentary infill of the offshore zone (minimum thickness of 10 m) was constructed. The
174 chronological framework of the sedimentary sequence of Lake Chungará was generated from 17 AMS
175 ^{14}C dates of bulk organic matter and aquatic plant macrofossils, and by one $^{238}\text{U}/^{230}\text{Th}$ date from
176 carbonates (see further details of age model in Giralt et al., 2008).

177 Samples for analyses were taken every 5-10 cm from core CHUN11A (Fig. 1). TC and total
178 inorganic carbon (TIC) content were measured using a UIC model 5011 CO₂ Coulometer, with TOC
179 determined by subtraction of TIC from TC. Total nitrogen (TN) was determined in a Variomax C/N
180 following the Dumas' method (Ma & Gutterson, 1970). BSi was extracted following the alkaline
181 leaching technique (Mortlock & Froelich, 1989), measuring the resulting extract by the molybdate blue
182 colorimetric method (Hansen & Grashoff, 1983) using an AutoAnalyser Technicon II. TOC, TIC and
183 TBSi results are expressed in the form of percent values of the sediment dry weight. For the
184 calculation of dry bulk densities the samples were dried to remove free water. Fluxes of TOC and BSi
185 to the sediments were estimated calculating mass accumulation rates (MARs, $\text{mg cm}^{-2} \text{yr}^{-1}$) by
186 multiplying their concentrations by the sediment dry densities and sedimentation rates at each depth.
187 By calculating the fluxes, the input of each component is independent of the effects of sediment
188 dilution (Boyle, 2001). Although neither percent values nor MARs can provide on their own precise
189 paleoproductivity reconstructions, their use in combination can help in the identification of the main
190 trends in productivity (Engstrom & Wright, 1984; Boyle, 2001).

191 Samples for diatom analysis were processed using standard techniques (Renberg, 1990). At least
192 400 valves were counted per sampled interval. All counts were made at X1000 with Nomarski
193 differential interference contrast optics. Diatom preservation was estimated using the *F* index (Flower
194 & Likhoshway, 1993). Identifications of diatom taxa were based upon the available diatom floras from
195 the region (Rumrich et al., 2000) and elsewhere (e. g., Krammer & Lange-Bertalot, 1986-1991; Lange-
196 Bertalot, 2000-2005). Raw valve counts were converted to percentage abundance data. All statistical

197 analyses were carried out on a diatom relative abundance matrix of those taxa attaining a frequency of
198 more than 2% in at least one sample. Data were transformed by square-root transformation. Definition
199 of the main Diatom Assemblage Zones (DAZs) was performed using stratigraphically constrained
200 cluster analysis based on squared Euclidean dissimilarity (CONISS, Grimm, 1987), as implemented in
201 Psimpoll 4.10 (Bennett, 2002). Zonations with variances that exceeded values generated by a broken-
202 stick model of the distribution of variance were deemed statistically significant (Bennett, 1996).

203 Ordination analyses (Detrended Correspondence Analysis-DCA, and Principal Component
204 Analysis-PCA) were conducted with the CANOCO 4.5 computer program (ter Braak & Smilauer, 1998)
205 to identify the main underlying environmental gradients explaining the variability of the diatom
206 abundance data (Jongman et al., 1987). Although a transfer function for ionic concentration and
207 salinity was developed in the near Bolivian Altiplano (Sylvestre et al., 2001), most of the taxa present
208 in Lake Chungará do not occur in that dataset, and it was not useful for quantitative
209 paleoenvironmental studies. Therefore, only qualitative diatom-based paleoenvironmental
210 reconstructions were performed, carefully informed by contemporary data on diatom ecology
211 (following Sayer et al., 2010). In this case, the qualitative approach was made on the basis of the
212 study of modern analogues in Lake Chungará (Dorador et al., 2003) and the nearby Lake Titicaca
213 (Theriot et al., 1985; Iltis, 1992; Servant-Vildary, 1992; Tapia et al., 2003, 2004). Diatom autoecologies
214 derived from a survey on the literature (e. g. Servant-Vildary & Roux, 1990; Gasse et al., 1995;
215 Sylvestre et al., 2001) have also been used.

216 A tentative qualitative lake-level curve was constructed combining the previous and new multiproxy
217 data. These included i) the abundances of euplanktonic vs. periphytic diatoms, ii) changes in the
218 lithofacies, particularly the presence of carbonates (Sáez et al., 2007), iii) oxygen isotopic data on
219 diatom frustules ($\delta^{18}\text{O}_{\text{diat}}$) for the late Glacial and early Holocene, with $\delta^{18}\text{O}_{\text{diat}}$ enrichments and
220 depletions mostly indicating low and high lake-levels, respectively (Hernández et al., 2013), iv) the
221 oxygen isotopic characterization of carbonates ($\delta^{18}\text{O}_{\text{carbonate}}$), starting to precipitate at 10,200 cal yr BP,
222 with $\delta^{18}\text{O}_{\text{carbonate}}$ depletions and enrichments indicating water volume increases, and more evaporated
223 waters, respectively (Pueyo et al., 2011), v) the abundances of *Myriophyllum* sp. and *Botryococcus*
224 *braunii* (Sáez et al., 2007), and vi) the moisture balance reconstruction of Giralte et al. (2008).

225

226 4. RESULTS

227 4.1 Diatom Assemblages

228 A total of 109 taxa have been identified. Percent abundance data of 21 common diatoms were
229 plotted stratigraphically (Fig. 3). The diatom record is dominated by euplanktonic diatoms (mainly
230 *Cyclostephanos andinus* and diatoms of the *Discostella stelligera* complex), with subdominant
231 freshwater tychoplanktonic and benthic taxa (mainly *Staurosira construens* aff. *venter*, *Cocconeis*
232 *placentula* and *Nitzschia tropica*). The diatom dissolution index *F* shows moderately well preserved
233 valves in Unit 1, whereas diatom dissolution effects were more prominent in Unit 2 (Fig. 3). The
234 broken-stick model of the distribution of variance allowed the definition of eight DAZs (Table 1 and Fig.
235 3).

236 Previous preliminary examination of smear slides (Hernández et al., 2008, 2011) did not allow
237 precise determinations at the species level. In this study, routine counts allowed taxonomic differences
238 to be identified in specimens of *Cyclostephanos andinus* in the laminated sediments. Whereas the
239 valves found in the green laminae could be ascribed to the published description of *Cyclostephanos*
240 *andinus* (Tapia et al., 2004), the larger specimens preserved in the white laminae showed striking
241 differences under the microscope. Later SEM ultrastructural examination of the valves confirmed the
242 uncertain taxonomic identity of the larger *Cyclostephanos andinus*, which in the future may be
243 assigned to a new closely related species (cf. Fritz et al., 2012) or, alternatively, may be considered
244 *Cyclostephanos andinus* of extreme morphology (Edward Theriot, pers. comm.). Until its taxonomic
245 affinity is affirmed, it will be referred to as *Cyclostephanos* cf. *andinus* in this publication.

246 A DCA was performed to estimate the length of the dominant gradient in the diatom assemblages
247 and to evaluate whether the taxa in the core samples followed a unimodal or linear distribution
248 (Jongman et al., 1987). Results indicated that the longest gradient was 2.08 SD units, suggesting a
249 linear response (Leps & Smilauer, 2003). For this reason a PCA was subsequently performed. During
250 the implementation of the PCA we wanted to restrict our analyses to the identification of the main long-

251 term environmental forcings on the composition of the diatom assemblages. However, the white and
252 light green laminae of Unit 1 (Facies A and B), made up of a quasi-monospecific assemblage of
253 *Cyclostephanos* cf. *andinus*, represented very short-term conditions (extraordinary diatom blooms)
254 interrupting any long term trend (Hernández et al., 2008, 2011). This taxon was not present in the
255 banded and massive Unit 2 (Facies D, E and F). To partial out the effects of both sources of variation,
256 we performed a Partial PCA using the lithological units (laminated, i. e., Unit 1, vs. non-laminated, i. e.,
257 Unit 2) as covariables (ter Braak & Smilauer, 1998; Leps & Smilauer, 2003). This procedure allows us
258 to ascertain whether there is still any environmental explanation of the long-term changes in the
259 diatom record once the effects of the short-term variability imposed by the white laminae are removed.

260 The first two principal components of the partial PCA (PC1 and PC2) explained 83.6% of the total
261 variance ($\lambda_1 = 0.625$; 69.4%, and $\lambda_2 = 0.128$; 14.2%). *Cyclostephanos andinus* shows the highest
262 score for the first main direction of variation (PC1), and the diatoms of the *Discostella stelligera*
263 complex acquiring the most negative score (Fig. 4). The second ordination axis (PC2) shows highest
264 scoring for *Cyclostephanos* cf. *andinus*, with most of the periphytic taxa (e. g. *Nitzschia tropica*,
265 *Staurosira construens* aff. *venter*, *Fragilaria capucina*) also showing positive scores. At the opposite
266 side of the gradient, *Cyclostephanos andinus* shows the most negative score. Variations of the first
267 two principal components throughout the core are plotted in the diatom abundance diagram (Fig. 3).

268

269 **4.2 Geochemical proxy data**

270 Depositional evolution of Lake Chungará has been reconstructed based on sedimentary facies
271 analyses and a number of geochemical proxies. The percent values and MARs of TOC and TBSi,
272 percent content of TIC, and the TOC/TN atomic ratio are plotted along with the percent abundance of
273 benthic diatoms, used here as a rough indicator of changes in water depth, and the scores of the first
274 two axis derived from the PCA conducted on the diatom abundance data (Fig. 5). Additionally,
275 previous isotopic data on organic matter, carbonates, and diatom frustules, and the percent
276 abundance of *Botryococcus braunii* observed in palynological slides (Sáez et al., 2007) are also
277 included.

278 4.2.1 Unit 1

279 TBSi content in Unit 1 is high, ranging from 41 to 54%. Fairly stable values in TBSi occur from the
280 bottom to 531 cm (c. 9,350 cal yr BP), comprising Subunit 1a and the lower part of Subunit 1b. The
281 fairly constant percent content of Subunit 1a and the lower part of Subunit 1b is, however, not mirrored
282 by TBSi MARs data, which show a rising trend from 6.6 mg TBSi cm² yr⁻¹ to a maximum flux for the
283 whole sedimentary record of 29.2 mg TBSi cm² yr⁻¹ recorded in Subunit 1a at 652 cm (c. 10,600 cal yr
284 BP). This trend is followed by a decline to a minimum value of 5.4 mg TBSi cm² yr⁻¹, which is again
285 not accompanied by significant variations in the percentage of TBSi. Maximum values for percent
286 content of TBSi are recorded in the top half Subunit 1b, with a maximum of 75% at 474 cm (c. 8,600
287 cal yr BP), declining afterwards. This rise is paralleled by an increase in the TBSi flux to the
288 sediments, which reached values as high as 19.2 mg TBSi cm² yr⁻¹.

289 Whereas TOC and TBSi MARs follow a similar pattern, other differences stand out, especially
290 when %TOC is considered. The bottom of Subunit 1a shows a declining trend in %TOC, followed by
291 an overall persistent rising trend throughout subunits 1a and 1b. This trend starts at 787 cm (c. 11,600
292 cal yr BP), when a minimum of 2.5% TOC is recorded, coinciding with the onset of the Holocene. The
293 highest values in the whole unit for TOC (8.3%) and its accumulation rate (4.0 mg TOC cm² yr⁻¹)
294 correspond to the 682 cm level (c. 10,950 cal yr BP), when a small decrease in both the content of
295 TBSi and its MAR is recorded. The TOC flux to the sediments declines after this peak, until a minimum
296 of 0.9 mg TOC cm² yr⁻¹ at 550 cm (c. 9,600 cal yr BP). %TOC shows, however, a general rising trend,
297 which fluctuates between 4.7 to 8.6%.

298 This unit ends at 450 cm (c. 8,300 cal yr BP) with a strong reduction in the flux of TBSi and TOC to
299 the sediments, as well as with the diminution of their percent content, which is concomitant with the
300 first occurrence of carbonate-rich layers and a sharp increase in %TIC (3.8%). Although a previous
301 TIC peak occurred at 550 cm (c. 9,500 cal yr BP) it was not associated to discrete carbonate laminae.

302 The atomic TOC/TN ratio shifts between 6.9 and 12.6 throughout this unit (a large fall at 712 cm, c.
303 11,000 cal yr BP, can certainly be attributed to an analytical error), and although a rising trend is
304 visible throughout subunits 1a to 1b, most of the values fall in the <10 range.

305 4.2.2 Unit 2

306 Unit 2 starts yielding flux values of 24.4 mg TBSi cm² yr⁻¹ and 3.6 mg TOC cm² yr⁻¹. After the %TIC
307 peak that separates Unit 1 and Unit 2, %TBSi rises to a maximum of 62.8 for the whole unit at 422 cm
308 (c. 8,000 cal yr BP), whereas %TOC also increases to 9.2 at the same level. Immediately after, there
309 is a declining trend from this level onwards, involving a sharp fall in the case of TBSi after 337 cm (c.
310 7,200 cal yr BP). TBSi MARs and %TBSi reach the lowest values for the whole record from this time
311 to present, with values that range between 1.8 to 8.8 mg TBSi cm² yr⁻¹ and 6.3 to 34.8%, respectively.
312 TOC fluxes are also strongly reduced, ranging from 0.4 to 2.5 mg TOC cm² yr⁻¹, but maintaining
313 values above those of the Late Glacial. In contrast, %TOC shows substantial fluctuations, with a peak
314 at 22 cm (c. 1,500 cal yr BP) of 9.7%. Reductions of TOC and TBSi content are, however, magnified
315 by the presence of tephra layers at 224, 56 and 39 cm. In spite of the general decrease in the
316 geochemical paleoproductivity proxies, a consistent rising trend is recorded between 308-255 cm (c.
317 6,900-6,400 cal yr BP), when %TBSi and %TOC show a parallel increase coincident with a maximum
318 value of 4.4 for TIC.

319 The TOC/TN curve shows oscillations throughout the record, although maintaining a general
320 increasing trend towards the present. This is most evident when the flux of TBSi is strongly reduced
321 after 337 cm (c. 7,200 cal yr BP). As is the case for %TBSi, %TOC and %TIC, there is also a
322 consistent increase in the TOC/TN ratio between 308-255 cm (c. 6,900-6,400 cal yr BP) when the
323 highest values for the whole record (14.0 and 14.5) are reached.

324

325 5. DISCUSSION

326 5.1 Meaning of the diatom assemblages

327 Lake Chungará has a diatom record characterized by shifting dominance of large vs. small taxa,
328 typified by *Cyclostephanos andinus* and *Discostella stelligera*, respectively. These are interrupted by
329 episodes of exclusive dominance of a very large diatom, *Cyclostephanos* cf. *andinus*, manifested in
330 the deposition of the white, beige, and very light green laminae. Both *Cyclostephanos andinus* and the

331 diatoms of the *Discostella stelligera* complex represent high lake-level conditions without elevated
332 concentration of salts (Tapia et al., 2003).

333 *Cyclostephanos* is a genus of euplanktonic diatoms characteristic of well-mixed waters under
334 isothermal conditions (Håkansson, 2002), whereas the diatoms of the *Discostella stelligera* complex
335 thrive well in stratified low energy environments (e. g. Rühland et al., 2008). Large cells, such as those
336 of *Cyclostephanos andinus* and *Cyclostephanos* cf. *andinus*, require well-mixed conditions to avoid
337 sinking in the water column (Margalef, 1978). On the other hand, their larger size increases their
338 nutrient requirements, and their low surface to volume area (S/V) reduces nutrient uptake. For these
339 reasons they only thrive well under high nutrient concentrations (Finkel et al., 2005; Litchman et al.,
340 2009). Conversely, enhanced buoyancy of small-sized phytoplankton, such as the components of the
341 *Discostella stelligera* complex, gives an advantage under thermal stratification, and their high S/V ratio
342 facilitates nutrient uptake under lower nutrient situations. Although other factors besides water column
343 mixing regime can simultaneously act to explain the abundances of centric diatoms in sedimentary
344 records (Saros & Anderson, 2014), comparison with modern analogues shows that ecophysiological
345 adaptations to avoid sinking are the most likely main driver of *Cyclostephanos* and *Discostella*
346 abundances in Lake Chungará. Diatoms of the *Discostella stelligera* group are currently more
347 abundant during the austral summer, when stratification is favored (Dorador et al., 2003). This taxon is
348 also most abundant in the nearshore regions of Lake Titicaca, where waters are warmer (Tapia et al.
349 2003). By contrast, *Stephanodiscus astraëa*, the former name for *Cyclostephanos andinus* (Theriot et
350 al., 1985; Tapia et al., 2004), was found as the main component of the phytoplankton assemblages in
351 the cold season, when mixing by isothermal conditions can be prompted (Dorador et al., 2003). This
352 result also fits with the known ecology of the species in Lake Titicaca, where it is associated with the
353 breakdown of thermal stratification and very high levels of nutrients (Theriot et al., 1985). Iltis (1992)
354 also reported blooms, when 100% of the diatom assemblage can be made up by *Cyclostephanos*
355 *andinus* (Servant-Vildary, 1992).

356 Results of the PCA indicate that changes in the water column mixing regime and depth are the
357 primary controllers of the composition of the diatom assemblages. PC1 mainly reflects variations in the
358 large centric diatom *Cyclostephanos andinus* relative to small diatoms of the *Discostella stelligera*

359 complex. Thus it measures the euplanktonic diatom size distribution, which is related to water
360 turbulence (Fig. 5). The high abundance of *Cyclostephanos andinus* throughout the history of the lake
361 suggests that intervals of isothermal mixing were persistent. Nevertheless, their duration varied in
362 comparison with the stratification periods, as indicated by fluctuations in the relative abundance of the
363 *Discostella stelligera* group.

364 Changes in water depth are suggested by PC2, since it reflects variation in a set of periphytic
365 diatoms (e. g. *Nitzschia tropica*, *Staurosira construens* aff. *venter*, *Fragilaria capucina*.), vs. the
366 euplanktonic *Cyclostephanos andinus* (Fig. 4). On the other hand, *Cyclostephanos* cf. *andinus* shows
367 a close relationship with periphytic taxa, which suggests that, although euplanktonic, it needs
368 moderately shallow waters to develop blooms. An association with shallow waters has also been
369 found for other large species of the *Cyclostephanos andinus* complex, which became extinct during
370 the Quaternary (Fritz et al., 2012) and by large sized cells of the nominate *Cyclostephanos andinus* in
371 Lake Titicaca (Servant-Vildary, 1992). Also, its very large size indicates not only a well-mixed water
372 column, but an enhanced nutrient storage capacity (Litchman et al., 2009). Thus, *Cyclostephanos* cf.
373 *andinus* superblooms, and therefore the deposition of the white laminae, would be triggered by
374 increased nutrient input during shallow water periods. A lamina by lamina isotopic diatom
375 characterization showed that deposition of the white laminae occurs mainly at times of increase in
376 $\delta^{18}\text{O}_{\text{diat}}$ values, indicating reduced external hydrologic inputs to the lake, and depletions in the $\delta^{13}\text{C}_{\text{diat}}$,
377 an indicator at this sampling scale of light carbon upwelled from the hypo- to the epilimnion
378 (Hernández et al., 2011). All these data support the interpretation of *Cyclostephanos* cf. *andinus* as a
379 suitable indicator of conditions when nutrients stored in the hypolimnion are released to the epilimnion
380 during relative lowstands that favor entrainment of hypolimnetic waters into surface waters.

381

382 **5.2 Paleoecological evolution of Lake Chungará and relationship with major climatic events**

383 Sedimentological, micropaleontological, and geochemical indicators were used to define the
384 depositional evolution of Lake Chungará and a qualitative paleohydrological history characterized by
385 several low and highstand phases during the period 12,400-1,300 cal yr BP (Figs. 5 and 6). The

386 multiproxy approach followed in this review also allowed us to identify up to seven distinct productivity-
387 related stages in the paleoenvironmental evolution of the lake.

388

389 5.2.1 Stage 1 (c. 12,400–12,100 cal yr BP)

390 Reduced productivity conditions are recorded at this initial stage, as indicated by the relatively low
391 fluxes of TOC and TBSi to the sediments (Fig. 5). Minimum depth conditions for the whole record were
392 reached (Fig. 6), as suggested by the highest percent abundance of benthic diatoms. Low lake-level is
393 supported by the presence of pollen belonging to the aquatic macrophyte *Myriophyllum* sp. and a very
394 low concentration of the chlorophycean *Botryococcus braunii* (Sáez et al., 2007). Although values of
395 PC1 suggest complete water column mixing to the bottom and nutrient release coherent with low lake-
396 level, cold conditions associated with the Late Glacial prevented high productivity, as the TOC and
397 TBSi MARs indicate.

398 5.2.2 Stage 2 (c. 12,100–10,800 cal yr BP)

399 This stage shows a significant reduction in benthic diatoms which, however, still maintain high
400 values, indicating that shallow waters persisted. A progressive increase in %TOC, starting at c. 11,400
401 cal yr BP, as well as the highest MARs values for TBSi and TOC, indicate a period of enhanced
402 productivity (Fig. 5), an interpretation also supported by the $\delta^{13}\text{C}_{\text{diat}}$ and $\delta^{15}\text{N}_{\text{org}}$ enrichments (Pueyo et
403 al., 2011; Hernández et al., 2013) (Fig. 5). This rise is concomitant with a sudden warming at the onset
404 of the Holocene (Thompson et al., 1998) and with increased nutrient inputs by runoff (highstand P1).

405 The *Discostella stelligera* complex dominated the first part of this stage (DAZ CHUN11A-02, Fig.
406 3), which suggests a stratified water column (Fig. 6). Relatively shallow waters during this first part of
407 this interval were, however, also favorable for the development of *Cyclostephanos* cf. *andinus*
408 superblooms, leading to the intermittent formation of white laminae (Facies A). The dominant stratified
409 conditions were therefore disturbed by sporadic and short-term episodes of strong turbulence. As the
410 change in the PC1 shows, the second part of this stage (most of DAZ CHUN11A-03) was
411 characterized by long periods of a well-mixed water column and high nutrients in surface waters,

412 concomitant with a peak in productivity conditions indicated by TOC and TBSi MARs (Fig. 5). The
413 change in the mixing regime is also reflected in the $\delta^{13}\text{C}_{\text{org}}$ depletion, which occurred between the two
414 parts of this period (Pueyo et al., 2011) and is likely related to the enrichment of the epilimnion with
415 light carbon under periods of enhanced mixing (Meyers, 1997; Cohen, 2003). The fact that the
416 magnitude of the $\delta^{13}\text{C}_{\text{diat}}$ enrichment does not keep pace with the increase in TOC and TBSi MARs
417 was also interpreted as an evidence of the intensification of mixing, since this would have released
418 isotopically depleted CO_2 from the hypolimnion, buffering the $\delta^{13}\text{C}_{\text{diat}}$ increase due to enhanced
419 productivity. Intermittent peaks in *Botryococcus braunii*, an indicator of increased water column-
420 stability (Margalef, 1983), suggest however a marked seasonality in the mixing regime.

421 Lake-level remained relatively shallow during this period, although a progressive rise is suggested
422 by the relative decrease in benthic diatoms. However, the paleohydrological change seems smaller
423 than further north, where wet conditions occurred in Lake Titicaca between c. 13,000 to 11,000 cal yr
424 BP (Baker et al., 2001; Tapia et al., 2003), correlating with the wet Coipasa lake cycle in most of the
425 Bolivian Altitplano (Servant et al., 1995).

426 5.2.3 Stage 3 (c. 10,800–10,000 cal yr BP)

427 This stage is characterized by a decrease in benthic diatoms after a significant peak at the onset of
428 this phase. Interestingly, the $\delta^{18}\text{O}_{\text{diat}}$ record during this interval shows an enrichment which is
429 contradictory with a highstand situation (Hernández et al., 2008) (Fig. 5). It was suggested that
430 flooding of the shallow east and south platforms (Fig. 1B) at this time increased the whole S/V ratio of
431 the lake, and therefore evaporation, explaining the $\delta^{18}\text{O}_{\text{diat}}$ enrichment. In this scenario, the peak in
432 benthic diatoms at the start of this stage could therefore be a product of not a lake-level drop, but a
433 consequence of the topographic effect of increased availability of shallow littoral habitats when the
434 flooding took place (Stone & Fritz, 2004; Wigdhal et al., 2014).

435 Flooding of the shallow platform is paralleled by two significant changes. On one hand, the
436 apparent decrease in productivity, as shown by the reduction in the TOC and TBSi MARs (Fig. 5). On
437 the other, the mixing status changes from well mixed, represented by the dominance of
438 *Cyclostephanos andinus*, to stratified conditions, represented by the dominance of the *Discostella*

439 *stelligera* group later on. In between this change, *Cyclostephanos* cf. *andinus* superblooms develop
440 and trigger white laminae deposition, as a consequence of easier nutrient recycling in now extensive
441 shallow areas of the lake.

442 Whereas the TOC flux declines, %TOC shows an increase during this stage (Fig. 5). The
443 postulated reduced mixing of the water column could have maintained low or anoxic conditions at the
444 lake bottom, as the values of $\delta^{13}\text{C}_{\text{carbonate}}$ around 7‰ also suggest (Pueyo et al., 2011) (Fig. 5). This
445 would increase organic matter preservation and therefore %TOC values. This organic matter is
446 predominantly of phytoplanktonic origin, as indicated by TOC/TN values around 10 (Meyers, 1997,
447 2003). The increase in %TOC, while %TBSi maintains similar levels, indicates a greater contribution of
448 the non-diatom component of the original phytoplanktonic community. This replacement of diatoms,
449 probably by motile phytoplankton, is what is expected with decaying turbulence (Margalef, 1978).

450 This stage coincides with declining summer insolation (Berger & Loutre, 1991) and a weakened
451 SASM concomitant with the northward ITCZ displacement (Haug et al., 2001; Cruz et al., 2005).
452 Under this scenario, a period of reduced moisture, and not a humid phase, would be expected in the
453 Andean Altiplano. ENSO variability has, however, been invoked to explain changes in moisture in the
454 tropical area during this period, so the recorded late Glacial to early Holocene humid conditions could
455 be triggered by the dominance of La Niña-like conditions at this time (Betancourt et al., 2000;
456 Koutavas et al., 2002; Hernández et al., 2010; Zech et al., 2010).

457 5.2.4 Stage 4 (c. 10,000–9,600 cal yr BP)

458 Benthic diatoms record their highest relative abundances in Holocene times during this stage,
459 suggesting a short-lived lowstand situation (Fig. 6). Lake-levels would be again similar to those of the
460 first part of stage 3 that maximized the extension of shallow habitats. The rise in the TOC/TN ratio
461 suggests increased contribution of the non-algal component, likely littoral macrophytes, to the organic
462 matter flux to the sediments. The peak in the abundance of the mesosaline *Nitzschia tropica* might
463 indicate a saline concentration associated with a decline in lake-level (e. g. Bao et al., 1999), a
464 common feature at present, when precipitation is reduced (Dorador et al., 2003). A carbonate peak
465 also occurs at this time. Intense photosynthetic activity during the superblooms of *Cyclostephanos* cf.

466 *andinus* is the most probable driver of carbonate precipitation by removal of CO₂ (Pueyo et al., 2011).
467 However, the decline in TOC and TBSi MARs suggests that although primary productivity was
468 extraordinarily high during the short-lived superblooms of *Cyclostephanos* cf. *andinus*, these had no
469 major effect in the total biomass production over the long term, which decreased during this stage.

470 During this event a significant change towards a more turbulent regime took place (Fig. 6). This
471 part of the sedimentary record exhibits the highest values of Mn, as recorded by XRF analyses
472 (Moreno et al., 2007). Mn precipitation usually indicates the oxygenation of a previously anoxic
473 hypolimnion (Cohen, 2003), suggesting that the well-stratified conditions during the previous Stage 3
474 would have produced seasonal or persistent anoxia, which is favorable for increased Mn concentration
475 in the water column.

476 The short-lived lowstand that characterizes this stage points to a dry event in the region. Additional
477 data on $\delta^{18}\text{O}_{\text{diat}}$ (Hernández et al., 2013), the development of brown-white interbedding and carbonate-
478 bearing laminated diatomite facies (Sáez et al., 2007), and high-resolution multiproxy geochemical
479 and mineralogical data (Giralt et al., 2008) supports this interpretation. The recorded fall in water level
480 matches with the summer insolation minimum at 10,000 yr (Berger & Loutre, 1991), which would favor
481 a northward shift of the ITCZ, a reduction in the strength of the SASM, and therefore a period of
482 reduced moisture (Garreaud et al., 2009). This short-lived dry period might be related to a similar
483 event detected in Lake Titicaca at approximately 11,000 to 10,000 cal yr BP (Baker et al., 2001; Tapia
484 et al., 2003). Uncertainties associated with age models constructed for lacustrine sequences in the
485 central Andean Altiplano (Quade et al., 2008), and different climatic responses due to latitudinal
486 effects (Abbott et al., 2003) might account for the observed differences in timing between the two
487 records. The Lake Pacucha sedimentary record from the Peruvian Andes (Hillyer et al., 2009) shows a
488 lowstand that peaked at c. 10,000 cal yr BP, closely fitting the shallow water conditions in Lake
489 Chungará.

490 5.2.5 Stage 5 (c. 9,600–7,400 cal yr BP)

491 This stage shows a significant lake-level rise (highstand P2) manifested by the very low percent
492 values of benthic diatoms and a $\delta^{18}\text{O}_{\text{diat}}$ depletion (Fig. 5). The record shows however a carbonate

493 precipitation peak at 8,300 cal yr BP, which is more probably related to Ca availability once prolonged
494 leaching of volcanic rocks in the catchment increased the concentration of Ca in lake waters (Pueyo et
495 al., 2011). Productivity is high, with a peak in %TBSi and increases in %TOC, as well as in TBSi and
496 TOC MARs. These conditions are also associated with $\delta^{13}\text{C}_{\text{org}}$ and $\delta^{15}\text{N}_{\text{org}}$ record peaks (Pueyo et al.,
497 2011) and a net increase in $\delta^{13}\text{C}_{\text{diat}}$, another indicator of elevated productivity at this time (Hernández
498 et al., 2013) (Fig. 5). The main factor responsible for high productivity may be enhanced nutrient
499 inputs from the catchment associated with increased water availability (Giralt et al., 2008). Lake water
500 rise, however, would have a counteractive effect, which is a restriction in the vertical mixing down to
501 the hypolimnion (Fig. 6). Weakly mixed waters prevailed during this stage, as indicated by a decrease
502 in the PC1 and the start of the steady increase of *Botryococcus braunii* (Fig. 5). This chlorophycean is
503 currently the main component of the phytoplankton in Lake Chungará during the warmest summers
504 when intense stratification develops (Dorador et al., 2003). The high values of $\delta^{13}\text{C}_{\text{org}}$ also recorded at
505 this time (Fig. 5) may not only be related to increased productivity, but also to enhanced stratification
506 that enriches DIC in ^{13}C (Meyers, 1997; Cohen, 2003). Because of reduced mixing and a deeper water
507 column, complete water column overturn would be hindered, preventing the necessary nutrient
508 release from the lake bottom that allows the maintenance of large centric diatoms. As a consequence
509 of the restriction in the lake's internal nutrient cycling, the *Cyclotella* cf. *andinus* superblooms
510 cease, and a transition from laminated (facies B) to massive (facies C) sediments occurs.

511 This humid phase can be ascribed to a wet period spanning 10,000 to 8,000 cal yr BP, when Lake
512 Titicaca showed overflowing lake-level conditions (Baker et al., 2001; Tapia et al., 2003). Both the
513 similar duration of this period in Chungará and Titicaca, and a similar time lag experienced by the
514 previous dry event, suggest that corresponds to the same phenomenon. Wetter conditions between
515 8,400-7,200 cal yr BP were also recorded in Lake Paco Cocha (Abbott et al., 2003). Shorter wet
516 episodes that also match in age with this Lake Chungará stage are known for Lake Pacucha (Hillyer et
517 al., 2009) at c. 8,730 and 8,300 cal yr BP, and Lake Potosí (Bolivia) at about 8,000 cal yr BP (Wolfe et
518 al., 2001).

519 5.2.6 Stage 6 (c. 7,400–3,550 cal yr BP)

520 This stage starts with a sharp increase in benthic diatoms and an enrichment in $\delta^{18}\text{O}_{\text{carbonate}}$, both
521 indicating a reduction in water depth (lowstand P3). The flux of TOC and TBSi is strongly reduced,
522 even to levels below those of the Late Glacial for TBSi. This is not accompanied by a decrease of the
523 same magnitude in TOC (Fig. 5). The observation of a much greater reduction in TBSi than in TOC in
524 both percent content and MARs suggests that other organisms are replacing in part the role of
525 diatoms as primary producers. *Botryococcus braunii* increases its abundance during this phase (Sáez
526 et al., 2007), and the TOC/TN ratio reaches the highest values for the whole record (Fig. 5). Both
527 observations support the idea that at least chloropyceans and macrophytes increased their
528 contribution to total primary productivity.

529 In spite of the strong reduction of the TBSi and TOC flux to the sediments, $\delta^{13}\text{C}_{\text{org}}$ maintained high
530 values during this phase (Pueyo et al., 2011). The carbonate-bicarbonate system in Lake Chungará is
531 currently dominated by HCO_3^- , with a molar distribution between free CO_2 , bicarbonate and carbonate
532 of 3:958:39 (Mülhauser et al., 1995). During long periods of stratification, rates of photosynthetic
533 inorganic carbon uptake can exceed rates of resupply of CO_2 , raising pH, but photosynthesis can
534 continue making use of bicarbonate or via carbon concentration mechanisms (Hopkinson et al., 2011).
535 Bicarbonate uptake by aquatic plants generally occurs when its concentration exceeds that of CO_2 by
536 more than ten times (Wetzel, 2001), a figure currently largely surpassed in Lake Chungará. Under
537 these circumstances, the carbon isotopic composition of algae becomes heavier (Meyers, 2003). This
538 could explain why there is a net increase in $\delta^{13}\text{C}_{\text{org}}$ values during this stage in spite of the strong
539 reduction in productivity. A rise in pH associated with alkalinizing base cations released by
540 volcanoclastic inputs during this phase (Sáez et al., 2007) could also explain a change to a
541 bicarbonate dominated system throughout this period. This hypothesis is also supported by the
542 general trend towards higher $\delta^{13}\text{C}_{\text{carbonate}}$ (Pueyo et al., 2011).

543 The diatom record shows a reduction in the *Discostella stelligera* group and sharp increase in
544 *Cyclostephanos andinus* during this phase, with both taxa codominating the assemblages (Fig. 3). A
545 less stable water column, and lowstand conditions facilitating a more complete overturn, favored
546 *Cyclostephanos andinus*. In spite of this, lowering of the lake water level never reached conditions that
547 allowed superblooms of *Cyclostephanos cf. andinus*. The codominance between the *Discostella*

548 *stelligera* group and *Cyclostephanos andinus* suggests that although water column-stability decreased
549 compared to the previous phase, thermal-stratification was very common. This is also supported by
550 the high percentages of *Botryococcus braunii*.

551 This stage fits into the mid-Holocene aridity period in the Altiplano, roughly established between
552 9,000 to 4,000 cal yr BP, but whose intensity and exact timing is variable over the region (Abbott et al.,
553 2003). Maximum aridity conditions are recorded in Lake Titicaca between c. 8,000 to 5,500 cal yr BP
554 (Baker et al., 2001). This time range resembles the dry phase in Lake Chungará from c. 7,400 to
555 3,600 cal yr BP. Uncertainties in our age model are greatly reduced after 8,000 cal yr BP (Giralt et al.,
556 2008), precluding a clear correlation with the chronology of Lake Titicaca. Lake Chungará record also
557 demonstrates that the mid Holocene period was not homogeneous, but fluctuating between dry and
558 wet conditions. The driest conditions would have developed between 7,400 and 6,600 cal yr BP
559 according to the diatom record, fitting with mineralogical and high-resolution XRF data (Giralt et al.,
560 2008). In contrast, a wetter period took place between c. 6,600 to 6,000 cal yr BP. This correlates with
561 a wet episode from 7,500 (7,000) to 6,500 (6,000) cal yr BP also recorded in Lake Titicaca (Baker et
562 al., 2001; Rowe et al., 2002; Tapia et al., 2003).

563

564 5.2.7 Stage 7 (c. 3,550–1,300 cal yr BP)

565 This stage is represented by the record of Subunit 2b, where volcanoclastic materials constitute a
566 great part of the sediments (Sáez et al., 2007). Marked fluctuations in %TOC and its MAR can partially
567 be an artifact due to the presence of tephras. There is, however, a consistent trend in the first part of
568 this stage to a general reduction in both TOC content and fluxes, as well as in the TOC/TN ratio. This
569 is coincident with a depletion in the $\delta^{18}\text{O}_{\text{carbonate}}$, interpreted as the end of the previous arid phase
570 (Pueyo et al., 2011). Because of this and the absence of any significant increase in the benthic diatom
571 content, changes reflected in the organic matter reaching the lake bottom at this time are likely due to
572 the increased contribution of allochthonous organic matter associated with enhanced runoff. The
573 reduction of *Cyclostephanos andinus* and the increase of the *Discostella stelligera* group point to a
574 strengthening water column stratification, likely associated to higher lake-levels (Fig. 6).

575 Sediment cores from lakes Titicaca, Lagunillas, and Umayo (Peru) show that this latest part of the
576 Holocene corresponds to a highstand phase (Rowe et al., 2002; Ekdahl et al., 2008). Establishment of
577 the over-flow conditions in lake Titicaca started after 4,000 to 3,100 cal yr BP (Baker et al., 2001;
578 Tapia et al., 2003), which match with the onset of this paleoproductivity stage in Lake Chungará.
579 Different lowstands have however been identified during this phase in Lake Titicaca, indicating that
580 this period was far from stable (Abbott et al., 1997; Baker et al., 2005). Similar fluctuations correspond
581 in Lake Chungará to small peaks in benthic diatoms at c. 2,800, 2,200 and 1,500 cal yr BP. Relatively
582 deeper waters at the coring site might probably have downweighted the magnitude of change in
583 benthic diatom abundance.

584

585 **5.3 Main drivers of long-term changes in biosiliceous productivity**

586 Paleoproductivity changes in Lake Chungará generally show a good agreement with the main
587 paleoclimatic phases defined in the central Andean Altiplano from a set of lacustrine records.
588 Climate has exerted a fundamental influence on changes in productivity, modifying allochthonous
589 nutrient inputs to the lake, as well as lake-levels and the water-column mixing regime. Changes in lake
590 morphometry associated to those lake-level fluctuations however modulated the magnitude of the
591 climate imprint in the sedimentary record.

592

593 *5.3.1 Nutrient availability associated with runoff*

594 Long-term variability in the external delivery of nutrients to the lake is the main responsible for
595 paleoproductivity changes. Periods of enhanced productivity (Stages 2, 5 and 7, Fig. 6) are coincident
596 with periods of increased runoff associated with elevated water availability in the Altiplano.
597 Conversely, at times of aridity (Stages 4 and 6, Fig. 6) the lake experienced reduced biomass
598 production. This is in agreement with the present-day pattern of phytoplanktonic biomass reduction that
599 accompanies water level falls in this lake (Dorador et al., 2003), and to the suggestion that the key

600 element controlling primary production in mountain lakes at time scales of a few decades to millennia
601 is the coupling of lake dynamics with the catchment biogeochemistry (Catalan et al., 2006).

602

603 5.3.2 Effects of lake morphometry on internal nutrient recycling

604 Nutrient availability is dependent not only on external inputs, but on internal recycling due to the
605 existing water column structure at a given time. Its change prompts shifts in phytoplankton
606 communities, which, in turn, affect primary productivity and higher trophic production (e. g., Margalef,
607 1978; Winder & Hunter, 2008). Three stages of well-stratified waters dominated by small-sized
608 diatoms of the *Discostella stelligera* group have been identified (Stages 3, 5 and 7, Fig. 6). Higher
609 turbulence and mixing is associated with four periods in which the large *Cyclostephanos* species are
610 more prominent (Stages 1, 2, 4 and 6, Fig. 6). The early phases in lake ontogeny (Stages 1 to 3, Fig.
611 6) show a clear correspondence between stronger mixing and elevated productivity, as shown by the
612 correspondence between PC1 and TBSi and TOC MARs. An exception is the Late Glacial (Stage 1,
613 Fig. 6) when, in spite of the dominance of isothermal conditions, productivity was low very likely due to
614 cold temperatures. The highest productivity conditions in the whole lake history were recorded when
615 increased turbulence is added to the effects of enhanced runoff (Stage 2, Fig. 6).

616 A major paleoecological transition takes place after Stage 3, when phases with nutrient recycling
617 by stronger turbulent conditions seem to be uncoupled from diatom productivity at the time scale of the
618 sediment record. This is shown by the existence of periods characterized by well stratified waters with
619 high productivity (Stage 5, Fig. 6) and others with less stratified conditions but reduced production
620 (Stages 4 and 6, Fig. 6). In the absence of reliable paleoindicators of factors that affect water
621 turbulence, such as wind stress, surface heat flux or turbidity currents, a very probable explanation for
622 this decoupling is that changes in lake basin morphometry adjust the effects of mixing (Imboden &
623 Wüest, 1995), causing a change in productivity levels. Lake Chungará shows a complex bottom
624 topography, combining steep shorelines with extensive shallow platform areas (Fig. 1B). The water
625 level fluctuations experienced during its history produced major changes in the relative extent of
626 potential deep mixing areas in the lake. During lowstands, complete or almost complete mixing of the

627 water column to the lake bottom is facilitated. When the ratio of the area of the epilimnion sediments
628 with respect to the total volume of the epilimnion is high, nutrient remineralization is rapid, enabling
629 nutrients to be circulated back into the epilimnion (Fee, 1979). During the early stages (stages 1 to 3,
630 Fig. 6) low water levels allow wind-driven turbulence to easily reach the nutrient-rich hypolimnion at
631 times of enhanced vertical mixing. This prompts productivity, temperature permitting. As the lake-level
632 rises during the early to the mid Holocene, complete vertical mixing becomes more restricted, and the
633 effects of periods of strong turbulence on diatom productivity intensification are reduced.

634 The combined effect of water mixing and lake morphometry on internal nutrient supply is
635 particularly well illustrated in the formation of the *Cyclostephanos* cf. *andinus* superblooms and,
636 therefore, on the deposition of white laminae in lithological Unit 1. White laminae are predominantly
637 formed during lowstand periods or when littoral platforms of the lake were flooded, forming extensive
638 shallow areas (Hernández et al., 2011). Under these circumstances, nutrient release from the lake
639 bottom is facilitated, triggering massive *Cyclostephanos* cf. *andinus* blooms. Maximum deposition of
640 white laminae is recorded during a particularly pronounced lowstand in stage 4 after a long oligomictic
641 to meromictic condition affected the lake (Fig. 6). The development of an oxygen-depleted
642 hypolimnion (Stage 3, Fig. 6) would enrich the bottom waters with phosphorous (Cohen, 2003), which
643 is ultimately released to the surface waters in the following stage, triggering the *Cyclostephanos* cf.
644 *andinus* superblooms. This mechanism explains the deposition of almost pure diatom oozes at times
645 of extended shallow conditions when, for this reason, the lake experiences a state of morphometric
646 eutrophy *sensu* Rawson (1955). This ephemeral condition, which relies on nutrient recycling from the
647 deep waters, has no great effect on the TBSi and TOC flux to the sediments in the long term (Fig. 5).
648 Yet, the importance of morphometric eutrophy should not be neglected when compared to the recent
649 parts of the record. Once a depth threshold is surpassed during the early to mid Holocene transition
650 (corresponding to the change from the laminated deposits of Unit 1 to the massive Unit 2), mixing
651 down to the bottom becomes more difficult, and the formation of the *Cyclostephanos* cf. *andinus*
652 superblooms is hindered. Any ulterior lowstand, such as those recorded during the mid-Holocene
653 aridity crisis, would have never put the lake-level below that depth threshold. Consequently,
654 productivity can no longer solely rely on internal nutrient recycling, and biosiliceous productivity falls to

655 minimum levels. Compared to lowstands associated to more juvenile stages in lake ontogeny, when
656 morphometric eutrophy was still possible, the TBSi flux is strongly reduced to levels below Late Glacial
657 times.

658 Surpassing the depth threshold likely not only brought about termination of the *Cyclostephanos* cf.
659 *andinus* superblooms, but also very probably produced the extinction of this taxon, which, so far, has
660 not been found at present in other lake systems of the central Andean Altiplano. Undescribed new
661 species of *Cyclostephanos* that went extinct have also been detected in Pleistocene sediments of
662 Lake Titicaca (Fritz et al., 2012). In Lake Chungará, as is true of Lake Titicaca, some of the putative
663 new morphospecies may be favored by conditions associated with shallower waters than the nominal
664 *Cyclostephanos andinus*.

665 5.3.3 Volcanism

666 The Lake Chungará record shows that it became increasingly dependent on allogenic controls on
667 its productivity during its evolution. Besides variations in runoff, another external forcing factor,
668 volcanic ash deposition, could have affected biosiliceous productivity. Increased silica loads
669 associated with ashfall during volcanic events have been reported as triggers of enhanced diatom
670 productivity in some lake systems (e. g. Lotter et al., 1995; Cruces et al., 2006). The most significant
671 change in Holocene volcanism in the area was the renewed activity of the Parinacota volcano after
672 7,500 cal yr BP (Giralt et al., 2008). However, in spite of increased silica availability by tephra
673 deposition during the sedimentation of Unit 2, biosiliceous productivity was significantly lowered in
674 Lake Chungará. Furthermore, no significant changes occurred in the diatom assemblages after the
675 different periods of tephra deposition. Yet, the relationship between tephra deposition and diatom
676 productivity is probably a time scale-dependent process. Some evidence points to short-term
677 reorganization of the diatom assemblages, as well as changes in productivity, after volcanic
678 disturbance, but these effects last for no more than 5 years (Cruces et al., 2006). Other observations
679 indicate that volcanic silica loads do not provide the necessary sustained stimulus to enhance
680 productivity, and that the long term trends in lake evolution are not fundamentally affected by tephra
681 inputs (Telford et al., 2004). A more detailed sampling would therefore be necessary to definitely

682 confirm the short-term consequences of airborne tephtras on the productivity conditions of Lake
683 Chungará.

684

685 **6. CONCLUSIONS**

686 The sedimentary record of Lake Chungará reveals a complex interplay between climatic and
687 lacustrine morphometric controls that influence paleoproductivity throughout its evolution. Precipitation
688 variability over the Andean Altiplano has been the most important primary forcing factor for changes in
689 allochthonous nutrient inputs and paleoproductivity during the studied period. The magnitude of
690 changes in climate-driven impacts on the aquatic system are, however, modulated by morphometry-
691 related in-lake controls that show that there is not a linear response of lacustrine productivity to
692 changes in precipitation and, therefore, to climatic variability.

693 Variations in the water-column mixing regime acted as a key driver in long-term productivity
694 conditions, compensating losses produced at times of decreased nutrient availability associated with
695 runoff. This is particularly well exemplified during the early Holocene (10,800-9,600 cal yr BP), which
696 includes two distinct paleoproductivity stages. During the first stage, the lake experienced dominant
697 oligo to meromictic conditions that, irrespective of intervals of enhanced precipitation in the Andean
698 Altiplano, lead to a significant decrease in productivity. During more arid phases in the early Holocene,
699 the trend toward decreased productivity was maintained. However, complete overturn, facilitated by a
700 lowstand situation, helped to sustain episodic moderate productivity conditions by nutrient recycling
701 from the sediments. When this morphometric eutrophy occurred, most of the biomass was produced by
702 episodic superblooms of a very large diatom, *Cyclostephanos* cf. *andinus*, which is strictly dependent
703 on the existence of deep water circulation and relatively shallow waters.

704 The effects of mixing of the water column therefore strongly depend on changes in the
705 morphometry of the lake basin associated with its evolution. Lake Chungará experienced a net long-
706 term lake-level increase since its origin up to c. 8,300 cal yr BP, when maximum depth conditions
707 were reached. Because of the complex topography of the basin, this lake-level increase substantially

708 modified the area of the epilimnion sediments with respect to the total volume of the epilimnion. Once
709 the depth threshold was surpassed, a deeper lake prevented complete mixing of the water column to
710 the bottom, and the episodic superblooms of *Cyclostephanos* cf. *andinus* were no longer possible.
711 This made the lake more dependent on allochthonous nutrient inputs and, therefore, on climate
712 variability. As a result, the Andean mid-Holocene Aridity Period, lasting in Lake Chungará from c.
713 7,400 to 3,550 cal yr BP, brought a sharp decrease in productivity which, at least for diatoms,
714 descended to levels below Late Glacial times. Crossing the depth threshold not only sharply
715 decreased the lake productivity, but was also accompanied by a reduction in the relative role of
716 diatoms as primary producers, and by a shift to a bicarbonate-dominated system. Subsequently,
717 biosiliceous productivity never reached the levels of previous stages in the ontogeny of the lake.

718 Our results show that in this closed high mountain lake climatic changes constitute the primary
719 driver in the long-term productivity conditions, but that the magnitude of change can be strongly
720 amplified or reduced by factors intrinsic to the lake that vary during its ontogeny. This needs to be
721 taken into account when interpreting lacustrine paleoproductivity records as evidences of late
722 Quaternary climatic changes.

723

724 **ACKNOWLEDGMENTS**

725 The Spanish Ministry of Science and Innovation funded the research through the projects
726 ANDESTER (BTE2001-3225), Complementary Action (BTE2001-5257-E), LAVOLTER (CGL2004-
727 00683/BTE), GEOBILA (CGL2007-60932/BTE) and CONSOLIDER-Ingenio 2010 GRACCIE
728 (CSD2007-00067). The Limnological Research Center (USA) provided the technology and expertise
729 to retrieve the cores. We are grateful to CONAF (Chile) for the facilities provided in Parque Nacional
730 Lauca. We are also indebt to Edward Theriot, who examined scanning electron microscope
731 micrographs of the *Cyclostephanos* making up the laminated unit. Manel Leira is also thanked for his
732 advice on statistical analyses.

733

734 REFERENCES

- 735
736 Abbott, M.B., Binford, M.W., Brenner, M., Kelts, K., 1997. A 3500 14C yr high-resolution record of
737 water-level changes in Lake Titicaca, Bolivia/Peru. *Quaternary Research* 47, 169-180.
- 738 Abbott, M.B., Wolfe, B.B., Wolfe, A.P., Seltzer, G.O., Aravena, R., Mark, B.G., Polissar, P.J., Rodbell,
739 D.T., Rowe, H.D., Vuille, M., 2003. Holocene paleohydrology and glacial history of the central
740 Andes using multiproxy sediment studies. *Palaeogeography, Palaeoclimatology and*
741 *Palaeoecology* 194, 123-138.
- 742 Anderson, N.J., 1995. Temporal scale, phytoplankton ecology and paleolimnology. *Freshwater Biology*
743 34, 367-378.
- 744 Baker, P.A., Fritz, S.C., Garland, J., Ekdahl, E., 2005. Holocene hydrologic variation at Lake Titicaca,
745 Bolivia/Peru, and its relationship to North Atlantic climate variation. *Journal of Quaternary Science*
746 20, 655-662.
- 747 Baker, P.A., Seltzer, G.O., Fritz, S.C., Dunbar, R.B., Grove, M.J., Tapia, P.M., Cross, S.L., Rowe,
748 H.D., Broda, J.P., 2001. The history of South American tropical precipitation for the past 25,000
749 years. *Science* 291, 640-643.
- 750 Bao, R., Sáez, A., Servant-Vildary, S., Cabrera, L., 1999. Lake-level and salinity reconstruction from
751 diatom analyses in Quillagua formation (late Neogene, Central Andean Forearc, northern Chile).
752 *Palaeogeography, Palaeoclimatology, Palaeoecology* 153, 309-335.
- 753 Bennett, K.D., 1996. Determination of the number of zones in a biostratigraphical sequence. *New*
754 *Phytol.* 132, 155-170.
- 755 Bennett, K.D., 2002. Documentation for Psimpoll 4.10 and Pscomb 1.03, C Programs for Plotting
756 Pollen Diagrams and Analysing Pollen Data. Uppsala University.
- 757 Berger, A., Loutre, M.F., 1991. Insolation values for the climate of the last 10 million years. *Quaternary*
758 *Science Reviews* 10, 297-317.
- 759 Betancourt, J.L., Latorre, C., Rech, J.A., Quade, J., Rylander, K.A., 2000. A 22,000-Year Record of
760 Monsoonal Precipitation from Northern Chile's Atacama Desert. *Science* 289, 1542-1546.
- 761 Boyle, J.F., 2001. Inorganic geochemical methods in paleolimnology, In: Last, W.M., Smol, J.P. (Eds.),
762 *Tracking Environmental Change Using Lake Sediments. Volume 2: Physical and Geochemical*
763 *Methods.* Kluwer Academic Publishers, Dordrecht, pp. 83-141.
- 764 Brylinsky, M., Mann, K.H., 1973. An analysis of factors governing productivity in lakes and reservoirs.
765 *Limnology and Oceanography* 18, 1-14.
- 766 Castañeda, I.S., Werne, J.P., Johnson, T.C., 2009. Influence of climate change on algal community
767 structure and primary productivity of Lake Malawi (East Africa) from the Last Glacial Maximum to
768 present. *Limnology and Oceanography* 54, 2431-2447.
- 769 Catalan, J., Camarero, L., Felip, M., Pla, S., Ventura, M., Buchaca, T., Bartomeus, F., De Mendoza,
770 G., Miró, A., Casamayor, E.O., Medina-Sánchez, J.M., Bacardit, M., Altuna, M., Bartrons, M.,
771 Díaz de Quijano, D., 2006. High mountain lakes: extreme habitats and witnesses of
772 environmental changes. *Limnetica* 25, 551-583.
- 773 Cohen, A.S., 2003. *Paleolimnology.* Oxford University Press, Oxford.
- 774 Cruces, F., Urrutia, R., Parra, O., Araneda, A., Treutler, H., Bertrand, S., Fagel, N., Torres, L., Barra,
775 R., Chirinos, L., 2006. Changes in diatom assemblages in an Andean lake in response to a recent
776 volcanic event. *Archiv Fur Hydrobiologie* 165, 23-35.
- 777 Cruz, F.W., Burns, S.J., Karmann, I., Sharp, W.D., Vuille, M., Cardoso, A.O., Ferrari, J.A., Silva Dias,
778 P.L., Viana, O., 2005. Insolation-driven changes in atmospheric circulation over the past 116,000
779 years in subtropical Brazil. *Nature* 434, 63-66.
- 780 Deevey, E.S., 1955. The obliteration of the hypolimnion. *Memorie dell'Istituto Italiano di Idrobiologia,*
781 *Suppl* 8, 9-38.
- 782 Dorador, C., Pardo, R., Vila, I., 2003. Variaciones temporales de parámetros físicos, químicos y
783 biológicos de un lago de altura: el caso del lago Chungará. *Revista Chilena de Historia Natural*
784 76, 15-22.
- 785 Ekdahl, E.J., Fritz, S.C., Baker, P.A., Rigsby, C.A., Coley, K., 2008. Holocene multidecadal- to
786 millennial-scale hydrologic variability on the South American Altiplano. *The Holocene* 18, 867-
787 876.
- 788 Engstrom, D.R., Fritz, S.C., Almendinger, J.E., Juggins, S., 2000. Chemical and biological trends
789 during lake evolution in recently deglaciated terrain. *Nature* 408, 161-166.
- 790 Engstrom, D.R., Wright Jr., H.E., 1984. Chemical stratigraphy of lake sediments as a record of

- 791 environmental change, In: Haworth, E.Y., Lund, J.W.G. (Eds.), Lake Sediments and
792 Environmental History. Leicester University Press, Leicester, pp. 11-68.
- 793 Fee, E.J., 1979. A relation between lake morphometry and primary productivity and its use in
794 interpreting whole-lake eutrophication experiments. *Limnology and Oceanography* 24, 401-416.
- 795 Finkel, Z.V., Katz, M.E., Wright, J.D., Schofield, O.M.E., Falkowski, P.G., 2005. Climatically driven
796 macroevolutionary patterns in the size of marine diatoms over the Cenozoic. *Proceedings of the*
797 *National Academy of Sciences* 102, 8927-8932.
- 798 Flower, R.J., Likoshway, Y., 1993. An investigation of diatom preservation in Lake Baikal, Fifth
799 Workshop on Diatom Algae, March 16-20, Irkutsk, Russia, pp. 77-78.
- 800 Fritz, S.C., Baker, P.A., Tapia, P., Spanbauer, T., Westover, K., 2012. Evolution of the Lake Titicaca
801 basin and its diatom flora over the last ~370,000 years. *Palaeogeography, Palaeoclimatology,*
802 *Palaeoecology* 317, 93-103.
- 803 Garreaud, R., Vuille, M., Clement, A.C., 2003. The climate of the Altiplano: observed current
804 conditions and mechanisms of past changes. *Palaeogeography, Palaeoclimatology,*
805 *Palaeoecology* 194, 5-22.
- 806 Garreaud, R.D., Vuille, M., Compagnucci, R., Marengo, J., 2009. Present-day South American climate.
807 *Palaeogeography, Palaeoclimatology, Palaeoecology* 281, 180-195.
- 808 Gasse, F., Juggins, S., Ben Khelifa, L., 1995. Diatom-based transfer functions for inferring past
809 hydrochemical characteristics of African lakes. *Palaeogeography, Palaeoclimatology,*
810 *Palaeoecology* 117, 31-54.
- 811 Giralt, S., Moreno, A., Bao, R., Sáez, A., Prego, R., Valero-Garcés, B., Pueyo, J., González-Sampériz,
812 P., Taberner, C., 2008. A statistical approach to disentangle environmental forcings in a
813 lacustrine record: the Lago Chungará case (Chilean Altiplano). *Journal of Paleolimnology* 40,
814 195-215.
- 815 Grimm, E.C., 1987. CONISS: a Fortran 77 program for stratigraphically constrained cluster analysis by
816 the method of incremental sum of squares. *Computers and Geosciences* 13, 13-35.
- 817 Håkansson, H., 2002. A compilation and evaluation of species in the general *Stephanodiscus*,
818 *Cyclostephanos* and *Cyclotella* with a new genus in the family Stephanodiscaceae. *Diatom*
819 *Research* 17, 1-139.
- 820 Hansen, H.P., Grashoff, K., 1983. Automated chemical analysis, In: Grashoff, M., Ehrhardt, M.,
821 Kremling, K. (Eds.), *Methods of Seawater Analysis*. Verlag Chemie, Weinheim, pp. 368-376.
- 822 Haug, G.H., Hughen, K.A., Sigman, D.M., Peterson, L.C., Rohl, U., 2001. Southward Migration of the
823 Intertropical Convergence Zone Through the Holocene. *Science* 293, 1304-1308.
- 824 Hernández, A., Bao, R., Giralt, S., Barker, P.A., Leng, M.J., Sloane, H.J., Sáez, A., 2011.
825 Biogeochemical processes controlling oxygen and carbon isotopes of diatom silica in Late Glacial
826 to Holocene lacustrine rhythmites. *Palaeogeography, Palaeoclimatology, Palaeoecology* 299,
827 413-425.
- 828 Hernández, A., Bao, R., Giralt, S., Leng, M.J., Barker, P.A., Pueyo, J.J., Sáez, A., Moreno, A., Valero-
829 Garcés, B., Sloane, H.J., 2008. The palaeohydrological evolution of Lago Chungará (Andean
830 Altiplano, northern Chile) during the Lateglacial and early Holocene using oxygen isotopes in
831 diatom silica. *Journal of Quaternary Science* 23, 351-363.
- 832 Hernández, A., Bao, R., Giralt, S., Sáez, A., Leng, M.J., Barker, P.A., Kendrick, C.P., Sloane, H.J.,
833 2013. Climate, catchment runoff and limnological drivers of carbon and oxygen isotope
834 composition of diatom frustules from the central Andean Altiplano during the Lateglacial and Early
835 Holocene. *Quaternary Science Reviews* 66, 64-73.
- 836 Hernández, A., Giralt, S., Bao, R., Sáez, A., Leng, M., Barker, P., 2010. ENSO and solar activity
837 signals from oxygen isotopes in diatom silica during late glacial-Holocene transition in Central
838 Andes (18°S). *Journal of Paleolimnology* 44, 413-429.
- 839 Herrera, C., Pueyo, J.J., Sáez, A., Valero-Garcés, B.L., 2006. Relación de aguas superficiales y
840 subterráneas en el área del lago Chungará y lagunas de Cotacotani, norte de Chile: un estudio
841 isotópico. *Revista Geológica de Chile* 33, 299-325.
- 842 Hillyer, R., Valencia, B.G., Bush, M.B., Silman, M.R., Steinitz-Kannan, M., 2009. A 24,700-yr
843 paleolimnological history from the Peruvian Andes. *Quaternary Research* 71, 71-82.
- 844 Hopkinson, B.M., Dupont, C.L., Allen, A.E., Morel, F.M.M., 2011. Efficiency of the CO₂-concentrating
845 mechanism of diatoms. *Proceedings of the National Academy of Sciences* 108, 3830-3837.
- 846 Hora, J.M., Singer, B.S., Wörner, G., 2007. Volcano evolution and eruptive flux on the thick crust of
847 the Andean Central Volcanic Zone: ⁴⁰Ar/³⁹Ar constraints from Volcán Parinacota, Chile.
848 *Geological Society of America Bulletin* 119, 343-362.
- 849 Iltis, A., 1992. Phytoplankton. Quantitative aspects and populations, In: Dejoux, C., Iltis, A. (Eds.),
850 *Lake Titicaca. A Synthesis of Limnological Knowledge*. Kluwer Academic Publishers, Dordrecht,

- 851 pp. 182-195.
- 852 Imboden, D.M., Wüest, A., 1995. Mixing mechanisms in lakes, In: Lerman, A., Imboden, D.M., Gat,
853 J.R. (Eds.), *Physics and Chemistry of Lakes*. Springer-Verlag, Berlin, pp. 83-138.
- 854 Johnson, T.C., Brown, E.T., McManus, J., 2004. Diatom productivity in northern lake Malawi during the
855 psat 25,000 years: implications for the position of the intertropical convergence zone at millennial
856 and shorter time scales, In: Battarbee, R.W., Gasse, F., Stickley, C.E. (Eds.), *Past Climate
857 Variability through Europe and Africa*. Springer, Dordrecht, pp. 932-116.
- 858 Jongman, R.H.G., ter Braak, C.J.F., van Tongeren, O.F.R., 1987. *Data Analysis in Community and
859 Landscape Ecology*. Pudoc, Wageningen, p. 299.
- 860 Koutavas, A., Lynch-Stieglitz, J., Marchitto, T.M., Sachs, J.P., 2002. El Niño-Like Pattern in Ice Age
861 Tropical Pacific Sea Surface Temperature. *Science* 297, 226-230.
- 862 Krammer, K., Lange-Bertalot, H., 1986-1991. Bacillariophyceae, In: Ettl, H., Gerloff, J., Heynig, H.,
863 Mollenhauer, D. (Eds.), *Süßwasserflora von Mitteleuropa*. Fischer-Verlag, Stuttgart.
- 864 Lange-Bertalot, H., 2000-2005. *Diatoms of the European Inland Waters and Comparable Habitats*.
865 Volumes 1, 2, 3, 4, 5. A. R. G. Gantner Verlag, Ruggell, Liechtenstein.
- 866 Leps, J., Smilauer, P., 2003. *Multivariate Analysis of Ecological Data using CANOCO*. Cambridge
867 University Press, Cambridge.
- 868 Litchman, E., Klausmeier, C.A., Yoshiyama, K., 2009. Contrasting size evolution in marine and
869 freshwater diatoms. *Proceedings of the National Academy of Sciences* 106, 2665-2670.
- 870 Lotter, A.F., Birks, H.J.B., Zolitschka, B., 1995. Late-glacial pollen and diatom changes in response to
871 two different environmental perturbations: volcanic eruption and Younger Dryas cooling. *Journal
872 of Paleolimnology* 14, 23-47.
- 873 Ma, T.S., Gutterson, M., 1970. Organic elemental analysis. *Analytical Chemistry* 42, 105-114.
- 874 Mackay, A.W., 2007. The paleoclimatology of Lake Baikal: A diatom synthesis and prospectus. *Earth-
875 Science Reviews* 82, 181-215.
- 876 Margalef, R., 1978. Life forms of phytoplankton as survival alternatives in an unstable environment.
877 *Oceanologica Acta* 1, 493-509.
- 878 Margalef, R., 1983. *Limnología*. Ediciones Omega, Barcelona.
- 879 Márquez-García, M., Vila, I., Hinojosa, L.F., Méndez, M.A., Carvajal, J.L., Sabando, M.C., 2009.
880 Distribution and seasonal fluctuations in the aquatic biodiversity of the southern Altiplano.
881 *Limnologica - Ecology and Management of Inland Waters* 39, 314-318.
- 882 Meyers, P.A., 1997. Organic geochemical proxies of paleoceanographic, paleolimnologic, and
883 paleoclimatic processes. *Organic Geochemistry* 27, 213-250.
- 884 Meyers, P.A., 2003. Applications of organic geochemistry to paleolimnological reconstructions: a
885 summary of examples from the Laurentian Great Lakes. *Organic Geochemistry* 34, 261-289.
- 886 Moreno, A., Giral, S., Valero-Garcés, B.L., Sáez, A., Bao, R., Prego, R., Pueyo, J.J., González-
887 Sampéiz, P., Taberner, C., 2007. A 14 kyr record of the tropical Andes: The Lago Chungará
888 sequence (18°S, northern Chilean Altiplano). *Quaternary International* 161, 4-21.
- 889 Mortlock, R.A., Froelich, P.N., 1989. A simple method for the rapid determination of biogenic opal in
890 pelagic marine sediments. *Deep-Sea Research* 36, 1415-1426.
- 891 Mühlhauser, H.A., Hrepic, N., Mladinic, P., Montecino, V., Cabrera, S., 1995. Water quality and
892 limnological features of the Andean Lake Chungará, northern Chile. *Revista Chilena de Historia
893 Natural* 68, 341-349.
- 894 Placzek, C., Quade, J., Betancourt, J.L., Patchett, P.J., Rech, J.A., Latorre, C., Matmon, A., Holmgren,
895 C., English, N.B., 2009. Climate in the dry central Andes over geologic, millennial, and
896 interannual scales. *Annals of the Missouri Botanical Garden* 96, 386-397.
- 897 Polissar, P.J., Abbott, M.B., Wolfe, A.P., Vuille, M., Bezada, M., 2013. Synchronous interhemispheric
898 Holocene climate trends in the tropical Andes. *Proceedings of the National Academy of Sciences*
899 110, 14551-14556.
- 900 Pueyo, J.J., Sáez, A., Giral, S., Valero-Garcés, B.L., Moreno, A., Bao, R., Schwalb, A., Herrera, C.,
901 Klosowska, B., Taberner, C., 2011. Carbonate and organic matter sedimentation and isotopic
902 signatures in Lake Chungará, Chilean altiplano, during the last 12.3 kyr. *Palaeogeography,
903 Palaeoclimatology, Palaeoecology* 307, 339-355.
- 904 Quade, J., Rech, J.A., Betancourt, J.L., Latorre, C., Quade, B., Rylander, K.A., Fisher, T., 2008.
905 Paleowetlands and regional climate change in the central Atacama Desert, northern Chile.
906 *Quaternary Research* 69, 343-360.
- 907 Rawson, D.S., 1955. Morphometry as a dominant factor in the productivity of large lakes.
908 *Internationale Vereinigung fuer Theoretische und Angewandte Limnologie Verhandlungen* 12,
909 164-175.
- 910 Renberg, I., 1990. A procedure for preparing large sets of diatom slides from sediment cores. *Journal*

- 911 of Paleolimnology 4, 87-90.
- 912 Risacher, F., Alonso, H., Salazar, C., 1999. Geoquímica de las aguas en las cuencas de cerradas: I, II
- 913 Regiones de Chile. Vol. II. Convenio de Cooperación DGA, UCN e IRD. Internal Report, p. 141.
- 914 Rowe, H.D., Dunbar, R.B., Mucciarone, D.A., Seltzer, G.O., Baker, P.A., Fritz, S., 2002. Insolation,
- 915 Moisture Balance and Climate Change on the South American Altiplano Since the Last Glacial
- 916 Maximum. Climatic Change 52, 175-199.
- 917 Rühland, K., Paterson, A.M., Smol, J.P., 2008. Hemispheric-scale patterns of climate-related shifts in
- 918 planktonic diatoms from North American and European lakes. Global Change Biology 14, 2740-
- 919 2754.
- 920 Rumrich, U., Lange-Bertalot, H., M., R., 2000. Diatomeen der Anden. Von Venezuela bis
- 921 Patagonien/Tierra del Fuego. A. R. G. Gantner Verlag K. G., Ruggell.
- 922 Sáez, A., Valero-Garcés, B.L., Moreno, A., Bao, R., Pueyo, J.J., González-Sampériz, P., Giral, S.,
- 923 Taberner, C., Herrera, C., Gibert, R.O., 2007. Lacustrine sedimentation in active volcanic
- 924 settings: the Late Quaternary depositional evolution of Lake Chungará (northern Chile).
- 925 Sedimentology 54, 1191-1222.
- 926 Saros, J.E., Anderson, N.J., 2014. The ecology of the planktonic diatom *Cyclotella* and its implications
- 927 for global environmental change studies. Biological Reviews, <http://doi.org/10.1111/brv.12120>.
- 928 Sayer, C.D., Davidson, T.A., Jones, J.I., Langdon, P.G., 2010. Combining contemporary ecology and
- 929 palaeolimnology to understand shallow lake ecosystem change. Freshwater Biology 55, 487-499.
- 930 Servant, M., Fournier, M., Argollo, J., Servant-Vildary, S., Sylvestre, F., Wirrmann, D., Ybert, J.P.,
- 931 1995. La dernière transition glaciaire/interglaciaire des Andes tropicales sud (Bolivie) d'après
- 932 l'étude des variations des niveaux lacustres et des fluctuations glaciaires. Comptes Rendus
- 933 Académie des Sciences Paris 320, 729-736.
- 934 Servant-Vildary, S., 1992. Phytoplankton. The diatoms, In: Dejoux, C., Iltis, A. (Eds.), Lake Titicaca. A
- 935 Synthesis of Limnological Knowledge. Kluwer Academic Publishers, Dordrecht, pp. 163-175.
- 936 Servant-Vildary, S., Roux, M., 1990. Multivariate analysis of diatoms and water chemistry in Bolivian
- 937 saline lakes. Hydrobiologia 197, 267-290.
- 938 Smol, J.P., 2008. Pollution of Lakes and Rivers. A Palaeoenvironmental Perspective. Blackwell
- 939 Publishing, Malden.
- 940 Sterner, R.W., 2008. On the Phosphorus Limitation Paradigm for Lakes. International Review of
- 941 Hydrobiology 93, 433-445.
- 942 Stone, J.R., Fritz, S.C., 2004. Three-dimensional modeling of lacustrine diatom habitat areas:
- 943 Improving paleolimnological interpretation of planktic : benthic ratios. Limnology and
- 944 Oceanography 49, 1540-1548.
- 945 Sylvestre, F., Servant-Vildary, S., Roux, M., 2001. Diatom-based ionic concentration and salinity
- 946 models from the south Bolivian Altiplano (15–23°S). Journal of Paleolimnology 25, 279-295.
- 947 Tapia, P.M., Fritz, S.C., Baker, P., Seltzer, G.O., Dunbar, R., 2003. A Late Quaternary diatom record
- 948 of tropical climatic history from Lake Titicaca (Peru and Bolivia). Palaeogeography,
- 949 Palaeoclimatology, Palaeoecology 194, 139-164.
- 950 Tapia, P.M., Theriot, E., Fritz, S.C., Cruces, F., Rivera, P., 2004. Distribution and morphometric
- 951 analysis of *Cyclostephanos andinus* comb. nov., a planktonic diatom from the Central Andes.
- 952 Diatom Research 19, 311-327.
- 953 Telford, R.J., Barker, P., Metcalfe, S.E., Newton, A., 2004. Lacustrine responses to tephra deposition:
- 954 examples from Mexico. Quaternary Science Reviews 23, 2337-2353.
- 955 ter Braak, C.J.F., Smilauer, P., 1998. CANOCO reference manual and user's guide to CANOCO for
- 956 Windows: Software for canonical community ordination (version 4). Microcomputer Power, Ithaca,
- 957 New York.
- 958 Theriot, E., Carney, H.J., Richerson, P.J., 1985. Morphology, ecology and systematics of *Cyclotella*
- 959 *andina* sp. nov. (Bacillariophyceae) from Lake Titicaca, Peru-Bolivia. Phycologia 24, 381-387.
- 960 Thompson, L.G., Davis, M.E., Mosley-Thompson, E., Sowers, T.A., Henderson, K.A., Zagorodnov,
- 961 V.S., Lin, P.-N., Mikhalevko, V.N., Campen, R.K., Bolzan, J.F., Cole-Dai, J., Francou, B., 1998. A
- 962 25,000-Year Tropical Climate History from Bolivian Ice Cores. Science 282, 1858-1864.
- 963 Wetzel, R.G., 2001. Limnology. Academic Press, San Diego.
- 964 Wigdahl, C.R., Saros, J.E., Fritz, S.C., Stone, J.R., Engstrom, D.R., 2014. The influence of basin
- 965 morphometry on the regional coherence of patterns of diatom-inferred salinity in lakes of the
- 966 northern Great Plains (USA). The Holocene 24, 603-613.
- 967 Winder, M., Hunter, D., 2008. Temporal organization of phytoplankton communities linked to physical
- 968 forcing. Oecologia 156, 179-192.
- 969 Wolfe, B.B., Aravena, R., Abbott, M.B., Seltzer, G.O., Gibson, J.J., 2001. Reconstruction of
- 970 paleohydrology and paleohumidity from oxygen isotope records in the Bolivian Andes.

- 971 Palaeogeography, Palaeoclimatology, Palaeoecology 176, 177-192.
972 Zech, J., Zech, R., May, J.-H., Kubik, P.W., Veit, H., 2010. Lateglacial and early Holocene glaciation in
973 the tropical Andes caused by La Niña-like conditions. Palaeogeography, Palaeoclimatology,
974 Palaeoecology 293, 248-254.
975 Zhou, J., Lau, K.M., 1998. Does a Monsoon climate exist over South America? Journal of Climate 11,
976 1020-1040.

977

978

979 **TABLE CAPTIONS**

980 **Table 1.-** Summarized description of diatom assemblage zones (DAZs) from Lake Chungará

981

982

983

984 **FIGURE CAPTIONS**

985 **Figure 1.-** A. Location of sites cited in this paper. B. Catchment and main topographical features of
986 Lake Chungará. Star indicates position of the studied core CHUN11A. The black line
987 correponds to the cross section (C) along the lake. C. Cross section of sediment infilling of
988 the lake. The position of the studied core is indicated by the sketch of the coring platform.
989 Lithological units according to Sáez et al. (2007).

990 **Figure 2.-** A. Digital DMT CoreScan (LRC, Minnesota) image of laminated sediments of core
991 CHUN11A. B. Micrograph (X100) of a petrographical thin-section showing a couplet made
992 up by a green (bottom) and a white lamina (top). C. Detail (X400) showing the white lamina
993 exclusively formed by skeletons of *Cyclostephanos* cf. *andinus*. D. *Idem* green lamina
994 dominantly made up by *Cyclostephanos andinus*, and some diatoms of the *Discostella*
995 *stelligera* complex embedded in an organic matter matrix.

996 **Figure 3.-** Diatom percentage diagram for selected taxa ($\geq 2\%$ abundance in at least one sample) of
997 Lake Chungará (core CHUN11A). Diatoms are grouped according to their habitat and
998 salinity preferences. Sample scores of the first two axis of the Principal Component
999 Analysis (PCA), and the diatom dissolution index F (Flower & Likhoshway, 1993), varying
1000 between 0 and 1, with values of $F=1$ indicating perfectly preserved valves, and $F=0$
1001 indicating that all valves show dissolution, are also plotted. Diatom Assemblage Zones
1002 (DAZs) generated by a broken-stick model of the distribution of variance (Bennett, 1996)

1003 and main lithological units and sedimentary facies according to Sáez et al. (2007) are also
1004 shown.

1005 **Figure 4.-** Principal Component Analysis (PCA) ordination biplot of samples (numbers) and diatom
1006 taxa (acronyms) in Lake Chungará. Achcon=*Achnanthes conspicua*, Amplib=*Amphora*
1007 *libyca*, Cocpla=*Cocconeis placentula*, Cycand=*Cyclostephanos andinus*,
1008 Cyyccfand=*Cyclostephanos* cf. *andinus*, Disste=*Discostella stelligera* complex,
1009 Fracap=*Fragilaria capucina* and varieties, Gommin=*Gomphonema minutum*,
1010 Navcry=*Navicula cryptotenella*, Navrad=*Navicula radiosa*, Navtri=*Navicula trivialis*,
1011 Navven=*Navicula veneta*, Navsem=*Naviculadicta seminulum*, Nittro=*Nitzschia tropica*,
1012 Opemut=*Opephora* sp. aff. *mutabilis*, Plalan=*Planothidium lanceolatum*,
1013 Staconv=*Staurosira construens* aff. *venter*, Staconc=*Staurosira construens* f. *construens*,
1014 Stacons=*Staurosira construens* f. *subsalina*, Stapin=*Staurosirella pinnata*, Ulnuln=*Ulnaria*
1015 *ulna*

1016 **Figure 5.-** Diatom and geochemical productivity-related proxies from core CHUN11A with indication of
1017 defined productivity stages and water level phases/events according to the constructed
1018 lake-level curve. Data are compared with the water availability curve of Giralt et al. (2008)
1019 and the insolation curve in austral summer at 18°S for the studied period (Berger & Loutre,
1020 1991). Proxies include sample scores for axis 1 (PC1) and axis 2 (PC2) of Principal
1021 Component Analysis on the diatom assemblages, percent of benthic diatoms, total
1022 biogenic silica (TBSi), total organic carbon (TOC), the TOC/total nitrogen atomic ratio
1023 (TOC/TN), and total inorganic carbon (TIC). TBSi and TOC are expressed as percent
1024 contents and mass accumulation rates (MARs). The figure also plots values of carbon and
1025 nitrogen isotopes on organic matter ($\delta^{13}\text{C}_{\text{org}}$, $\delta^{15}\text{N}_{\text{org}}$) and carbonates ($\delta^{18}\text{O}_{\text{carbonate}}$,
1026 $\delta^{13}\text{C}_{\text{carbonate}}$) (Pueyo et al., 2011), diatom frustules ($\delta^{18}\text{O}_{\text{diat}}$, $\delta^{13}\text{C}_{\text{diat}}$) (Hernández et al.,
1027 2013), as well as abundances of the chlorophycean *Botryococcus braunii* (Saéz et al.,
1028 2007). All data are plotted against age (cal yr BP).

1029 **Figure 6.-** Sedimentary and paleoecological model for Lake Chungará evolution in the period 12,400
1030 to 1,300 cal yr BP, with description of the defined paleoproductivity stages. See detailed
1031 explanation in text.

DIATOM ASSEMBLAGE ZONE	MAIN TAXA	OVERALL TRENDS
Depth (cm) Age (cal yr BP)		
CHUN11-01 860.7 - 835.2 12,400 – 12,100	Dominated by <i>Cyclostephanos andinus</i> and <i>Staurosira construens</i> aff. <i>venter</i> . Other tycho planktonic (mainly <i>Fragilaria capucina</i> and varieties) and benthic (mainly <i>Nitzschia tropica</i> , <i>Cocconeis placentula</i> and <i>Opephora</i> sp. aff. <i>mutabilis</i>) taxa appear in the record	Codominance of benthic and planktonic diatoms in a oligosaline waterbody of shallow but open waters
CHUN11-02 835.2 – 729.5 12,100 – 11,100	The assemblage is dominated by fluctuating numbers of diatoms of the <i>Discostella stelligera</i> complex (26.3 – 87.4%) with <i>Cyclostephanos andinus</i> , <i>Cyclostephanos</i> cf. <i>andinus</i> and the tycho pelagic <i>Staurosira construens</i> aff. <i>venter</i> as subdominant taxa	Shift to deeper and predominantly low mixing water conditions
CHUN11-03 729.5 – 627.9 11,100 – 10,450	<i>Cyclostephanos andinus</i> is the dominant taxa, reaching its maximum value (89.2%). The <i>Discostella stelligera</i> complex disappears, except in the interval 693.9 – 683.8 cm. <i>Cyclostephanos</i> cf. <i>andinus</i> shows episodic peaks. Moderate increase of the subdominant <i>Staurosira construens</i> aff. <i>venter</i> and the benthic <i>Cocconeis placentula</i> . Decline of <i>Nitzschia tropica</i>	Water shallowing with episodes of a strong turbulent regime
CHUN11-04 627.9 – 587.2 10,450 – 10,000	Marked increase of the <i>Discostella stelligera</i> complex, dominating almost the entire assemblage (82.6 – 94.2 %). <i>Cyclostephanos andinus</i> and <i>Cocconeis placentula</i> are a minor component of the zone	Deeper and stable water conditions
CHUN11-05 587.2 – 540.3 10,000 - -9,500	Starts with a sharp increase in <i>Cyclostephanos andinus</i> , decreasing afterwards. This decrease is paralleled by an increase in <i>Cyclostephanos</i> cf. <i>andinus</i> , which dominates the assemblage, and by <i>Staurosira construens</i> aff. <i>venter</i> and <i>Cocconeis placentula</i> . The <i>Discostella stelligera</i> complex acquire low percentages. Reappearance of <i>Nitzschia tropica</i>	Shift to a turbulent regime accompanied by a decrease in water level. Slight salinization
CHUN11-06 540.3 – 344.0 9,500 – 7,400	The <i>Discostella stelligera</i> complex dominates almost the entire assemblage (67.1 – 95.3%) reaching a maximum in the whole record. <i>Cyclostephanos andinus</i> shows low values (5.0 – 23.4%), and <i>Cyclostephanos</i> cf. <i>andinus</i> disappears in the record. <i>Cocconeis placentula</i> decreases	Lake deepening with a predominantly non-turbulent regime. The reduction in the oligosaline diatoms points to a salt dilution
CHUN11-07 344.0 – 61.8 7,400 – 2,600	<i>Cyclostephanos andinus</i> and the diatoms of the <i>Discostella stelligera</i> complex show fluctuating values codominating the assemblage. The epiphytic <i>Cocconeis placentula</i> increases	Moderate lake shallowing allowing macrophytic development. Shift to moderate mixing conditions
CHUN11-08 61.8 – 14.3 2,600 – 1,300	Sharp increase in the <i>Discostella stelligera</i> complex (74.2 – 87.0%) followed by a decline in <i>Cyclostephanos andinus</i> . <i>Cocconeis placentula</i> becomes a minor component of the assemblage	Maximum lake level situation, with the development of a predominantly stable water column

Figure
[Click here to download high resolution image](#)

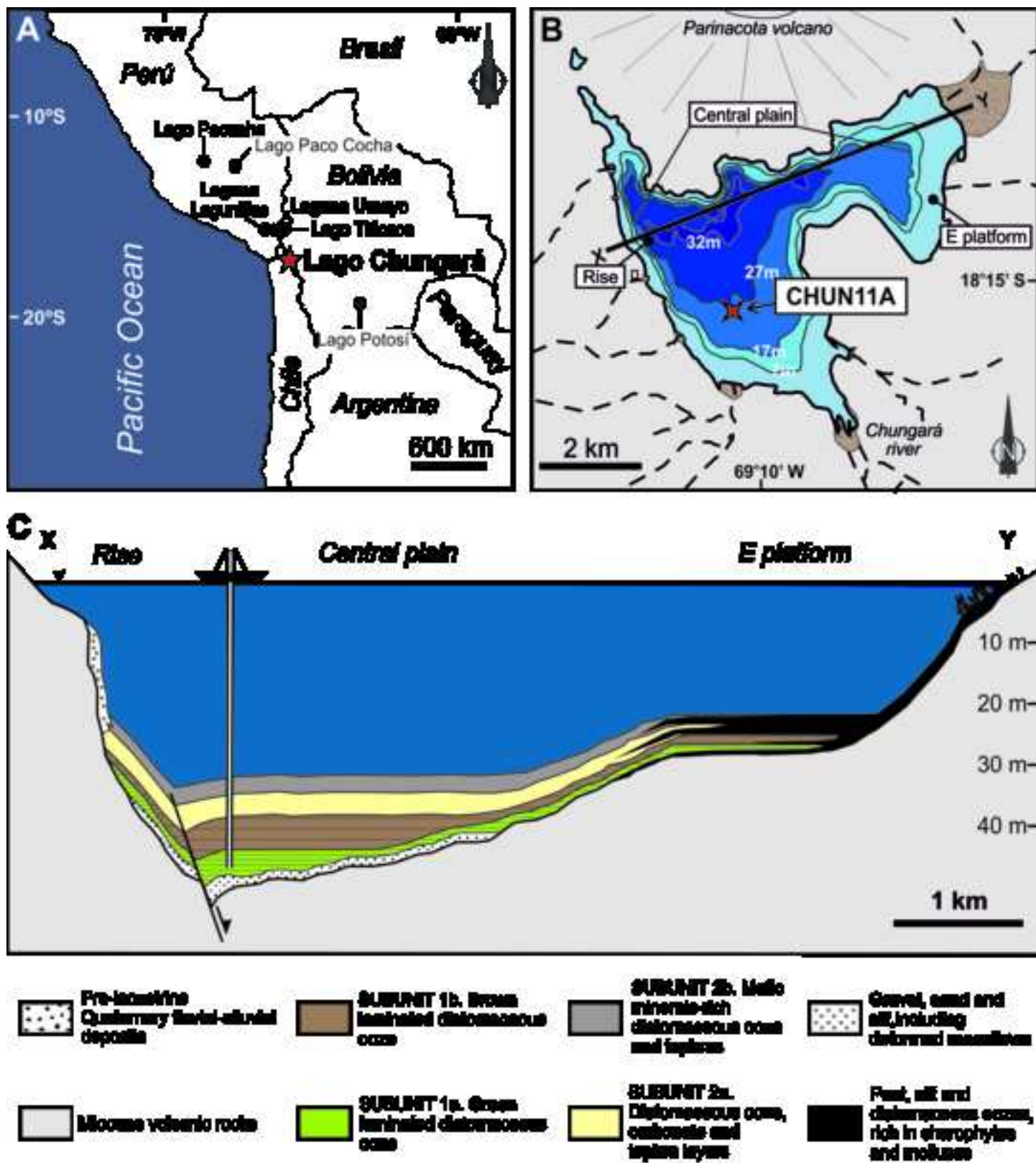


Figure 1

Figure

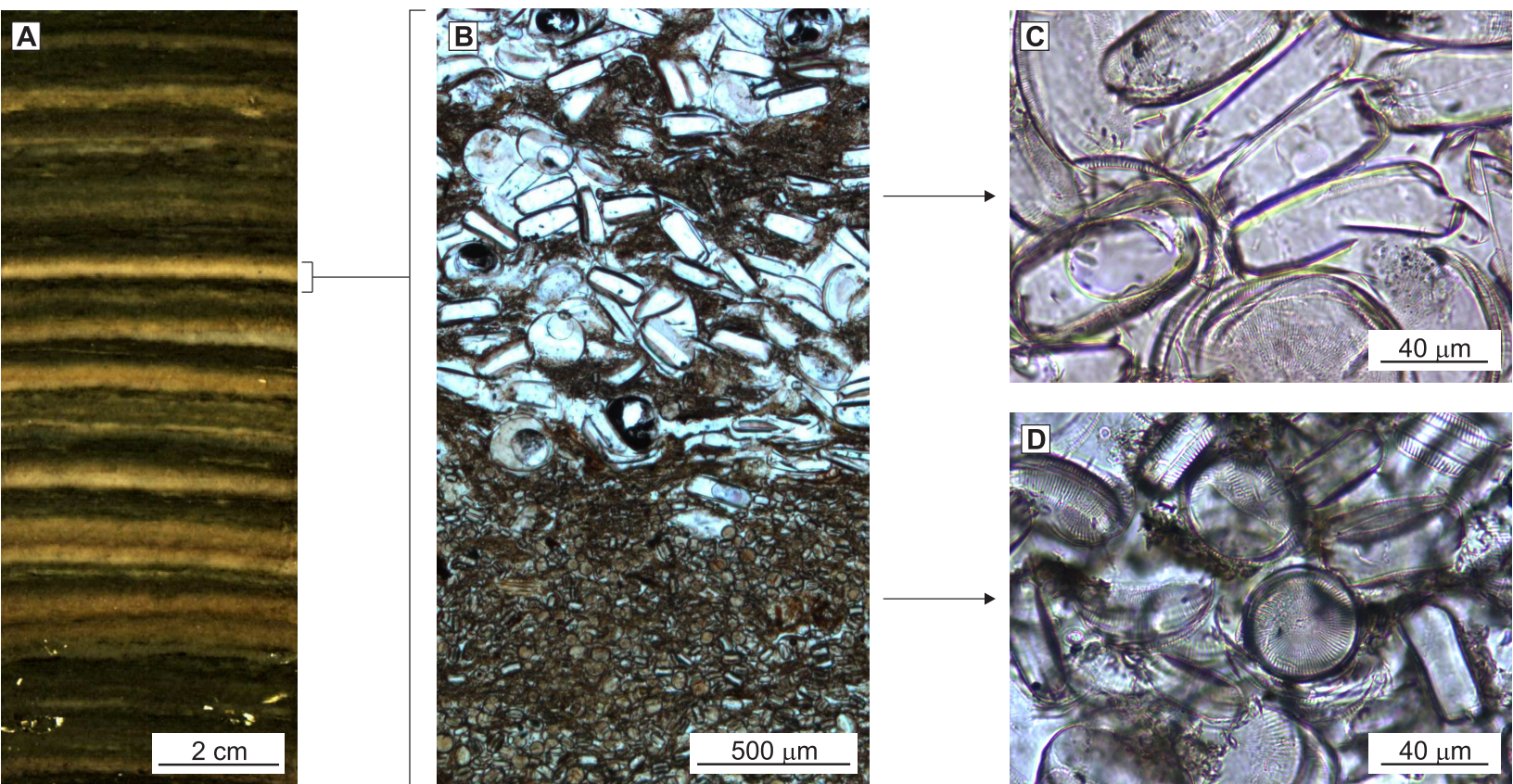


Figure 2

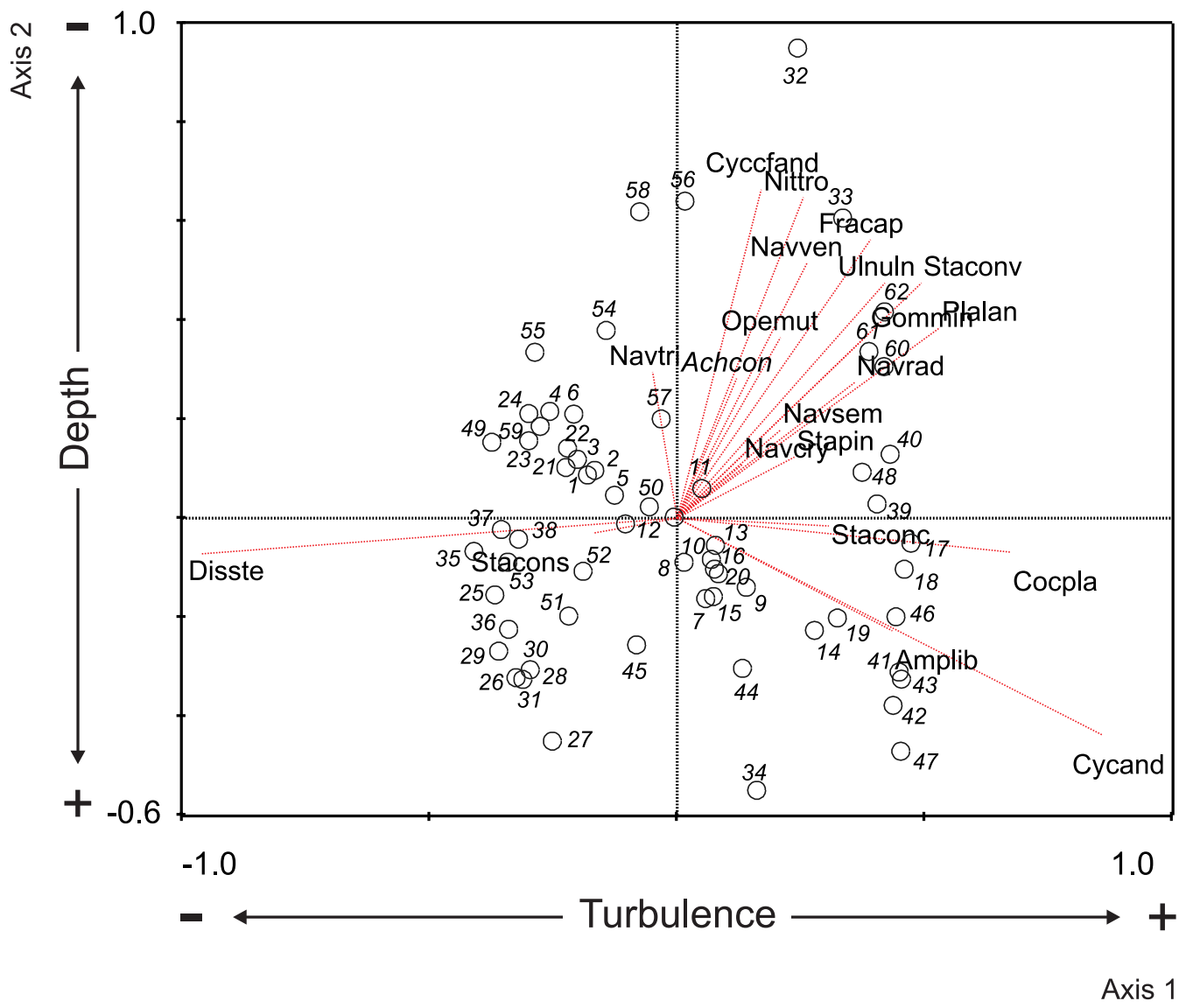


Figure 4

Figure

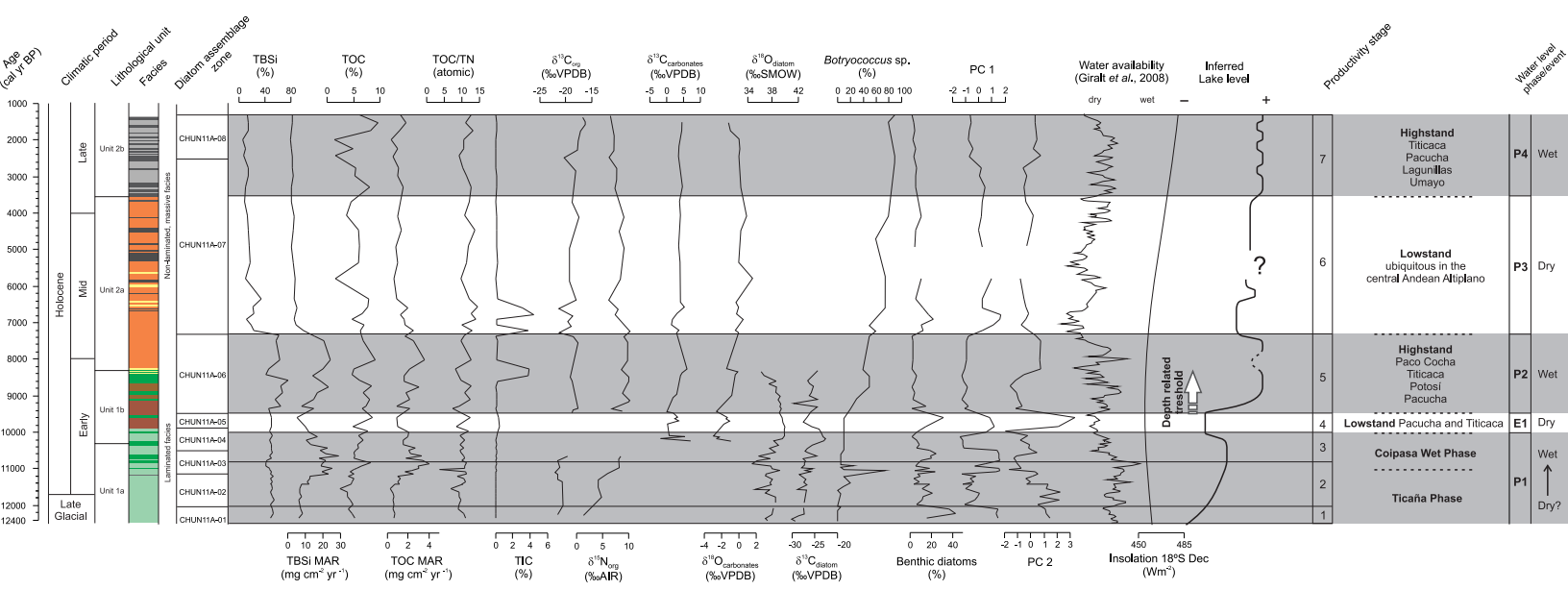


Figure 5

Figure

[Click here to download high resolution image](#)

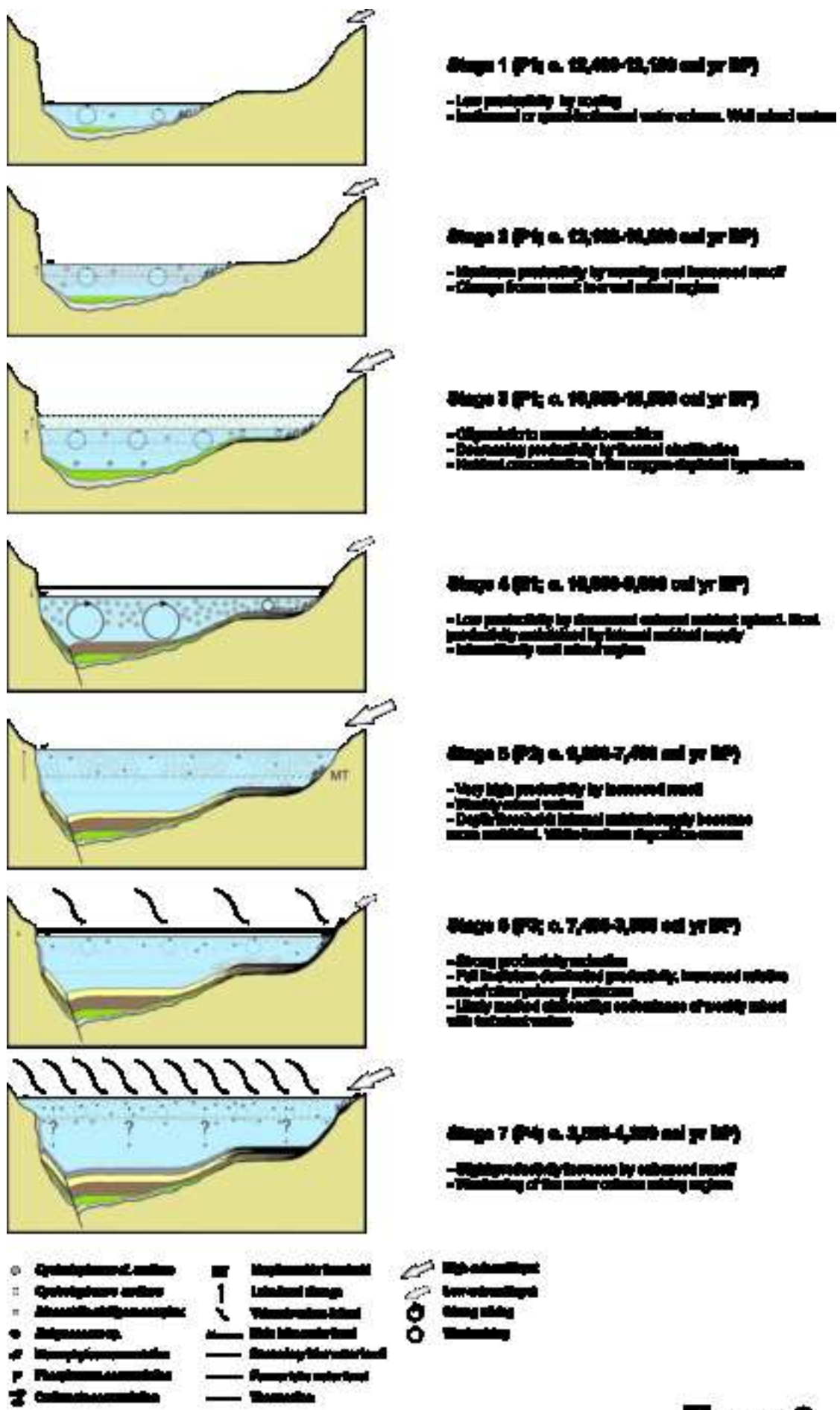


Figure 6